Generic Films and Fibers from Polysaccharides: Chitosan and Alginate

by

Ramiz Boy

A thesis submitted to the Graduate Faculty of
Auburn University
in partial fulfillment of the
requirements for the Degree of
Master of Science

Auburn, Alabama
August 06, 2011

Keywords: Polysaccharides, chitosan, alginate, biomaterials

Approved by

Maria L. Auad, Chair, Professor of Polymer and Fiber Engineering
Roy Broughton, Jr., Professor Emeritus of Polymer and Fiber Engineering
Peter Schwartz, Professor of Polymer and Fiber Engineering

Abstract

Chitosan and alginate are both extracted from natural resources, and both are biocompatible, biodegradable, and hydrophilic. Thus, chitosan-alginate biopolymer mixtures have the potential to form new functional polymers towards better performance, which can be utilized in different applications. Chitosan-alginate polymer films and fibers were prepared. Possible interactions and the effects of each component were investigated.

Miscibility, thermal stability, mechanical, and morphological properties of chitosan-alginate films were studied. We found that the film with ratio of 60:40 chitosan to alginate has the highest modulus and the highest tensile strength. The film with 80% chitosan content shows antibacterial activity. Furthermore, we developed a novel method to form wet-spun chitosan-alginate fibers with no additive and analyzed their mechanical and morphological properties. Roughness of the fibers increased with more chitosan content which reversely affected the tenacity.

Acknowledgments

I would like to express my sincere thanks to my advisor, Dr. Maria L. Auad, for her guidance and patience throughout this work. I am grateful to Dr. Roy Broughton, Jr. for his contribution and critical suggestions. I would also thank Dr. Peter Schwartz for being committee members and reviewing my research. Thanks to the Department of Polymer and Fiber Engineering for providing support and welcoming environment. I also would like to mention that this research would not have been possible without the support of Ministry of Turkish National Education.

I am most grateful to my family who have supported me and provided motivation all along my life. I would like also to thank all my friends who have helped me along this research.

Table of Contents

List of Tables

List of Figures

List of Abbreviations

CH Chitosan

AL Alginate

MMW Medium Molecular Weight

LMW Low Molecular Weight

ζ Zeta Potential

NMR Nuclear Magnetic Resonance Spectroscopy

UV-VIS Ultra Violet-Visible Spectroscopy

FTIR Fourier Transform Infrared

TGA Thermal Gravimetric Analysis

DSC Differential Scanning Calorimetry

DMA Dynamic Mechanical Analysis

SEM Scanning Electron Microscopy

E’ Storage modulus

MPa Megapascal

kDa Kilodalton

ASTM American Society for Testing and Materials

CHAPTER ONE

INTRODUCTION

1.1 LITERATURE REVIEW

1.1.1 Polysaccharides

Applications of polymers have been exploited in almost all disciplines of medicine, from complex tailored implants to drug delivery materials and practical devices situated outside the body (Dumitriu, 2002). Because every medical application is designed with its particularly specialized needs, a wide array of materials including high biocompatibility but distinct chemical and physical characteristics must be present (Dumitriu, 2002).

Most of the carbohydrate materials in nature exist in the form of polysaccharides (d'Ayala et al., 2008). They exhibit ideal biocompatibility and biodegradability, which are the fundamental characteristics for polymers exerted as biomaterials (Dumitriu, 2002). In addition, polysaccharides are not only involved in those substances just composed of glycosidically linked sugar structures, but also molecules that contain polymeric saccharide backbones linked via covalent bonds to amino acids, peptides, proteins, lipids, and other structures (d'Ayala et al., 2008). They possess various properties not available in other naturally occurring polymers, such as proteins and nucleic acids

(Dumitriu, 2002). Lately, several classes of polysaccharides have been applied for specific properties of antivirals, antitumorals, and gene modulators (Dumitriu, 2002).

Polysaccharides, also known as glycans, are composed of mono-saccharides and their derivatives (d'Ayala et al., 2008). If a polysaccharide comprises only one type of monosaccharide molecule, it is called homo-polysaccharide, or homoglycan, while the ones which have more than one type of monosaccharide are hetero-polysaccharides (d'Ayala et al., 2008). The well-known component of polysaccharides is D-glucose (Figure 1.1) – besides, D-fructose, D-galactose, L-galactose, D-mannose, L-arabinose, and D-xylose are also common (d'Ayala et al., 2008).

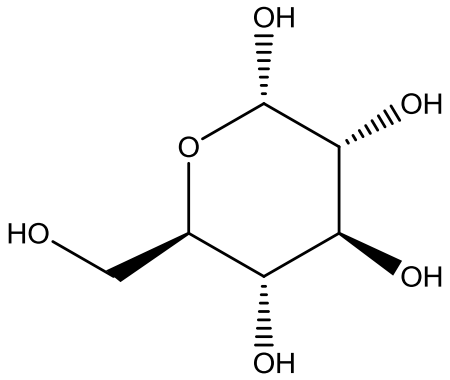

Figure 1. 1 Structure of D-glucose

Some monosaccharide derivatives occurred in polysaccharides contains the amino sugars (D-glucosamine and D-galactosamine) as well as their derivatives (*N*-acetylneuraminic acid and *N*-acetylmuramic acid), and simple sugar acids (glucuronic and iduronic acids). Homo-polysaccharides are often identified for the sugar unit they have; therefore, glucose homo-polysaccharides are called glucans, whereas mannose homo-polysaccharides are mannans. Polysaccharides vary in the character of their

component monosaccharides, in the length of their chains and in the amount of chain branching that occurs. Even though any sugar residue possesses only one anomeric carbon and also can form only one glycosidic linkage with hydroxyl groups on other molecules, each sugar residue carries several hydroxyls, one or more of which may be an acceptor of glycosyl substituents. This enables them to form branched structures that separates polysaccharides from proteins and nucleic acids, which occur only as linear polymers (d'Ayala et al., 2008).

The significant functions of polysaccharides in nature are either storage or structural purposes (d'Ayala et al., 2008). The prevalent storage polysaccharide in plants is starch, which occurs in two types: α-amylose and amylopectin. Structural polysaccharides display properties which differ considerably from those of the storage polysaccharides, while the structures of these two classes are similar. The structural polysaccharide cellulose (Figure 1.2) is the most abundant natural polymer on earth. Cellulose, exists in the cell walls of almost all plants as well as marine algae, is one of the main components, which gives physical structure and strength. Cellulose of animal origin derived from marine, tunicin, extracted from tunicates – invertebrate sea animals – is a choice of material, since it is highly crystalline (Cima et al., 1996, d'Ayala et al., 2008, Krishnan, 1975).

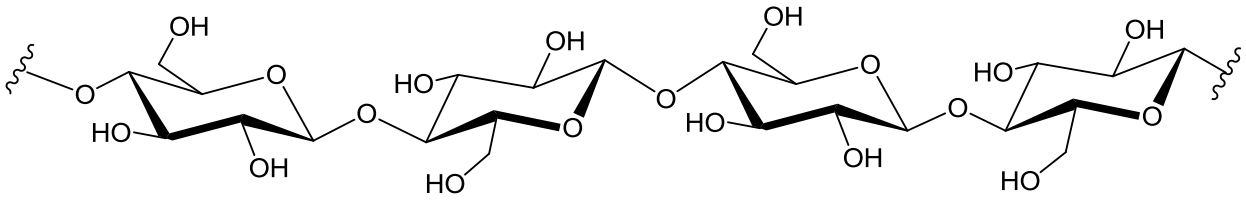

Figure 1. 2 Cellulosic chain formed from condensed D-glucose

Algal origin polysaccharides consist of alginates, agar and carrageenans. Agar (or agar-agar) is an unbranched polysaccharide acquired from some species of red algae's cell wall, primarily from the genuses *Gelidium* and *Gracilaria*, or seaweed, largely utilized as gelatin and thickener in food industry, and as a gel for electrophoresis in microbiology. It is chemically formed by galactose sugar molecules; that is the primary structural support for the algae's cell walls. Carrageenans are polysaccharides of galactan with alternating 1,3- and 1,4-linked galactose residues, which appear between the cellulosic plant structure of seaweeds. They are consumed in the food processing industry for their gelling, thickening, and stabilizing properties (d'Ayala et al., 2008).

Following cellulose, chitin is the second most common organic compound in nature. Chitin is widely distributed in marine invertebrates, insects, fungi, and yeast but does not occur in higher plants and higher animals (d'Ayala et al., 2008, Ehrlich et al., 2007).

Among polysaccharides that perform structural functions in nature, in this literature review, we will mainly focus on alginate and chitin's derivative chitosan. They are substantial not only as plentiful resources, but mainly for their appealing biological properties and potential in such fields mentioned above.

1.1.2 Polysaccharide Mixtures

1.1.2.1 Binary mixtures

Research on binary mixtures of polysaccharides has garnered much attention for more than two decades (Morris, 1998). A multitude of combinations of mixed polysaccharides make it impractical to analyze all such research. However, it is practical to classify binary mixtures in some simple kinds of gel (Morris, 1998). When two polysaccharides are blended together and then the mixture becomes gelled, a number of gel structure form, varying the chemistry of components, the rate and extent of polymer mixing, and the process of gelation (Cairns et al., 1987). Classification of these gels enables one to comprehend the elemental interrelationships among the properties of mixed gels and their constituents (Morris, 1998). This also offers to anticipate which kinds of analysis is needed to determine the structures of these gels (Morris, 1998).

These gel structures can be divided into four types (Cairns et al., 1987): swollen networks, phase separated networks, interpenetrating networks, and coupled networks (Figure 1.3). Swollen networks occur while one of the constituents of the mixture is forming a network and the other constituent occupies within and swells the network (Figure 1.3(a)). Interpenetrating networks are composed of two separated networks and each of them is dispersed in the total volume and interpenetrating through each other (Figure 1.3(b)). Phase separated networks are formed through mixing incompatible polysaccharides (Morris, 1998). This kind of gelation results in a composite or filled gel (Figure 1.3(c)). The coupled network is the most intriguing binary gel system, in which new heterotypic junction zones result on binding of two distinct polysaccharides (Figure 1.3(d)).

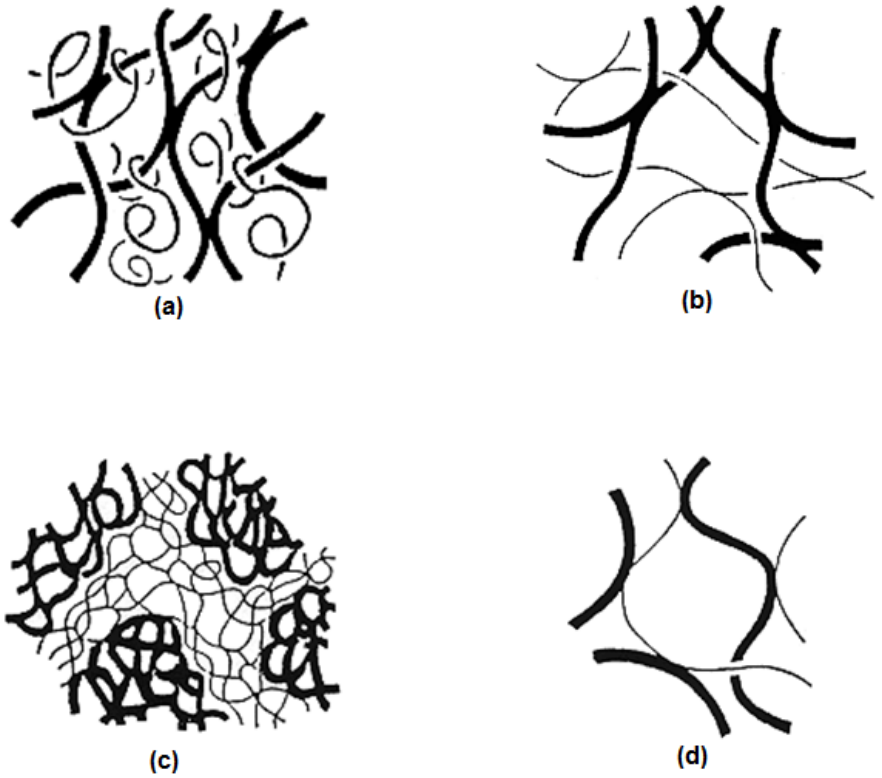

Figure 1. 3 Types of binary polysaccharide gel-structure: Polysaccharide A (■), polysaccharide B (—) (a) single polymer network containing the second polymer within the gel (swollen network), (b) interpenetrating networks, (c) phase-separated networks, (d) coupled network

The models exhibited in Figure 1.3 are likely to occur in a binary mixture. However, a given type of gel network should not be virtually always expected (Morris, 1998). For instance, two different polysaccharides can form an interpenetrating network at certain concentration of both polysaccharides but at very high ratios of the constituents, or at low enough concentrations of the two polymers, one or both of the constituents might be inadequate to create a network in all over sample volume (Morris, 1998).

1.1.2.2 Phase separated gels

Phase separated mixed gels usually comprise a continual phase and a supporting phase having inclusions in one another (Durrani and Donald, 1994). These systems exhibit a phase inversion at a given concentration at which the main constituent in the continual and supporting phases switch over.

Although mixed gels contain a high ratio of solvent (water), conventional polymer blends and mixed gels have some parallelism and functional similarities. This analogy inspired Clark et al. (1983) to develop a model which correlates a relationship between the modulus of a phase separated mixed gel and the volume fraction of the two component polymers in each phase. The model based on Takayanagi's approach (1963) was to calculate the modulus of a binary polymer blend (Clark et al., 1983).

A major problem in the analysis of phase separated biopolymer networks is the detection of any phase separation, unless separation is formed on a relatively bulk scale through the inclusion of two different layers (Durrani and Donald, 1994). It is unlikely to detect independently phase separated regions in a clear macroscopic single phase system either by visual inspection or by optical microscopy when the refractive indices of the two polymers in solution are not clearly distinctive (Durrani and Donald, 1994).

1.1.3 Polyelectrolyte Complexation

These complexes are composed of the assembly of two or more compatible polymers and may result from supramolecular interactions such as electrostatic effects, hydrophobic forces, hydrogen bonding, van der Waals forces, or combinations of these interactions (Dumitriu, 2002, Scranton et al., 1992, Tsuchida et al., 1982). The mechanism of complexation has a strong effect on the polymer solubility, rheology, conductivity, and turbidity in solutions.(Dumitriu, 2002, Scranton et al., 1992).

Polyelectrolyte complexes are mainly formed by electrostatic forces. Poly(cation)/poly(anion) pairs are constituted by proton transfer from acidic polymers to compatible basic polymers. Besides interpolymer complexes, research on intrapolymer complexes of polyampholytes has been done (Scranton et al., 1992). In these systems, polymer complexes may occur between reversely charged components of one polymer chain, or more specifically on the same monomer unit of that polymer (Dumitriu, 2002).

Finally, multivalent ions or polyelectrolyte itself may bind other polyelectrolytes in solution to form gels or coacervates (Chatterjee et al., 1987, Dumitriu, 2002). In addition, charge density, solvent, ionic strength, pH, and temperature also affect the formation and stability of complexation (Dumitriu, 2002). Insolubility of complexes is dependent upon the high charge density of polyelectrolytes (Dumitriu, 2002). Properties of the polyelectrolyte complexes are mainly tuned by the molecular weight of polymers including their cooperative interactions, concerted interactions, steric compatibility, and micro-environmental effects (Dumitriu, 2002, Kubota and Kikuchi, 1998).

1.1.4 Polysaccharides as Biometarials

1.1.4.1 Alginate

Alginate, a water-soluble linear binary copolymer, is isolated from brown seaweed and consists of alternating blocks of 1–4 linked α-L-guluronic acid (G) and β-D-mannuronic acid (M) residues with randomly alternating composition and sequence (Draget et al., 2009, George and Abraham, 2006). Figure 1.4 displays the structures of mannuronic and guluronic acid residues and the links between these residues in alginate. Due to the particular shapes of the monomers and their manner of linkage in the polymer, the geometries of the G-block parts, M-block parts, and alternating parts are significantly discrete (George and Abraham, 2006). Specifically, the G-blocks are clasped whereas the M-blocks possess a shape proposed to be an extended ribbon. A diamond shaped hole results in if two G-block regions are aligned side by side. The dimensions of so-called hole are ideal for the collective binding of calcium ions. The homo-polymeric regions of β-D-mannuronic acid blocks and α-L-guluronic acid blocks are inter-dispersed with regions of alternating structure (β-D-mannuronic acid–α-L-guluronic acid blocks) (Haug and Larsen, 1962, Haug et al., 1967). The arrangement and size of the orders and the molecular weight determine the physical properties of the alginates.

(I)

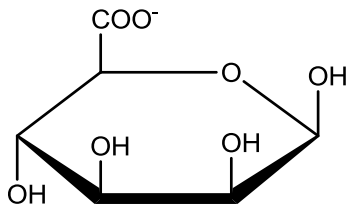

β-D-mannuronate (M)

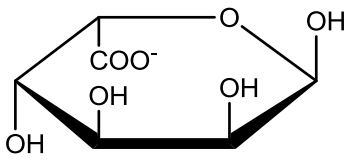

α-L-guluronate (G)

(II)

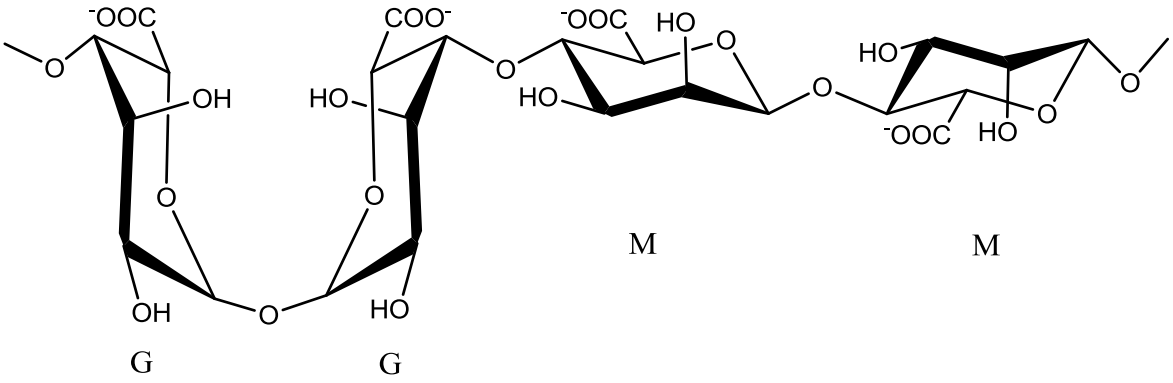

(III) MMMMMGGGGGGMGMGGGGGGGGGMGMGMGMG

M-block G-block G-block MG-block

Figure 1. 4 Chemical structure of alginates: (I) Alginate monomers, (II) chain conformation, (III) block distribution.

Regarding their molecular weights, alginates, similar to other polysaccharides, are polydisperse (Draget et al., 2009). This may be induced by polysaccharides which are indirectly coded for by the DNA, but are separated by polymerase enzymes and extraction may cause depolymerization. As a result of their polydispersity, an average value of the molecular weight is taken.

In terms of the source of alginates, commercial ones are derived from three species of brown marine algae (George and Abraham, 2006). These are Laminaria hyperborean, Ascophyllum nodosum, and Macrocystis pyrifera; in which alginates constitute up to 40% of the dry weight (Smidsrød and Skjaok-Brk, 1990, Sutherland, 1991). The structural composition and its sequential order might alter dependent on seasonal and ambient growing conditions (Haug, 1964, Indergaard and Skjåk-Bræk, 1987). Alginate occurs as a mixed salt of various cations encountered in the seawater such as Mg^{2+}, Sr^{2+}, Ba^{2+}, and Na^{+}. Bacterial alginates have also been extracted from Azotobacter vinelandii and several Pseudomonas species.

Figure 1. 5 Brown seaweed

The process of alginate extraction is basically a procedure of ion-exchange (Sime, 1990). The seaweed (Figure 1.5) is milled and washed. Then through a strong alkali and heat treatment, the extraction continues with the solution of sodium alginate. Alginate is precipitated in that solution with the addition of calcium chloride forming calcium alginate. A further acid treatment is applied to convert calcium alginate into alginic acid which finally can be treated to produce various forms of commercial alginates (Sime, 1990). For example,

1) Treatment with sodium carbonate or other bases to fabricate alginate salts
2) Reaction with propylene oxide to fabricate propylene glycol alginate

The process of alginate's gelation can be performed under an extraordinarily mild conditions and by using non-toxic reactants (George and Abraham, 2006). The most substantial property of alginate is its ability to form gels by reaction with multivalent cations such as Ca^{2+}. Hyrogels as well as beads, fibers and films of alginate can be made by extruding a solution of sodium alginate into a divalent cross-linking solution, such as Ca^{2+}, Sr^{2+}, or Ba^{2+} (George and Abraham, 2006). Monovalent cations and Mg^{2+} ions do not cause gelation (George and Abraham, 2006, Rees and Welsh, 1977). The gelation and cross-linking of the polymers are mostly accomplished through the replacement of sodium ions on the guluronic acids with the divalent cations, and the packing of these guluronic groups to form the characteristic egg-box structure shown in Figure 1.6.

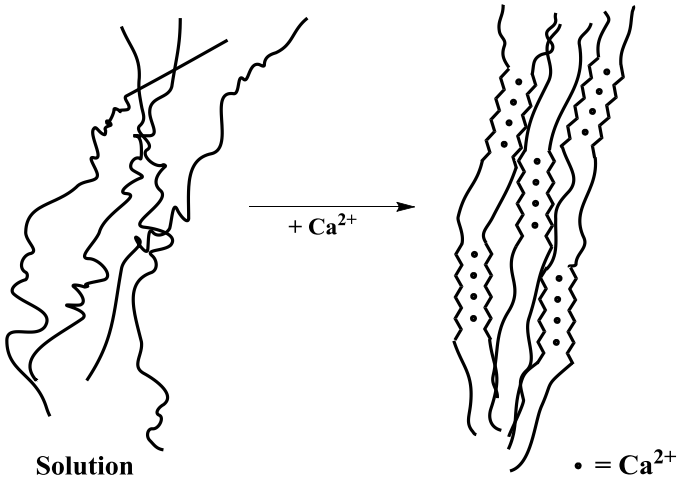

Figure 1. 6 Egg-box structure of an alginate gel formed by gelation of Ca^{2+} ions

The segments of poly-L-guluronate display an intensified binding of the divalent cations over a chain length of 20 monomers (Sime, 1990, Smidsrød and Skjaok-Brk, 1990). This indicates that gelation mechanism occurs in a cooperative manner in the gelation process in which binding sites are already arranged in an ordered array and binding of one ion helps to bind the next. These impacts are not seen for poly-D-mannuronic acid or alternating sequences (Morris et al., 1973, Sime, 1990).

Each alginate chain dimerizes to form joints with many other chains and therefore gel networks are formed (Dupuy et al., 1994, George and Abraham, 2006). So the calcium reactivity of alignment is the result of calcium-induced dimeric association of the G-block regions (George and Abraham, 2006). These hydrogels that are similar to solids in maintaining their forms and resisting stress possess 99–99.5% water with rest being alginate (George and Abraham, 2006). Upon the amount of calcium involved in the system, these inter-chain connections can be either impermanent or permanent (George and Abraham, 2006). Impermanent connections are acquired by low amounts of calcium, giving rise to highly viscous, thixotropic solutions (George and Abraham, 2006). Precipitation or gelation results from permanent connections of the chains at higher calcium amounts (George and Abraham, 2006). A great deal of research has proved that the chemical composition, molecular size, the hydrogel forming kinetics and the cation have a significant impact on some of its functional properties including porosity, swelling behavior, stability, biodegradability, gel strength, and the gel's immunological characteristics and biocompatibility (George and Abraham, 2006).

Alginate and its gels have been used in numerous and markedly different applications. It has historically been most commonly exerted in the food industry (Augst

et al., 2006). It has also been utilized as a stabilizer and an emulsifier, e.g., in low-fat fat substitutes, on account of its intrinsic properties and the interactions of alginate with proteins, fats, or fibers (Augst et al., 2006). Alginate is also found utility as a gelling agent for food products, since alginate–pectin mixtures gel independently of sugar content, and its use can bear low-calorie products (Augst et al., 2006). Alginate is chemically modified with propylene glycol to allow its application under acidic conditions (Draget et al., 2005, Glicksman, 1987), and to bind flaked, chunked, or milled foodstuffs. It is also a shear-thinning agent in the textile/paper-printing industry due to its high hue yield and print levelness (Glicksman, 1987, McLachlan, 1985). In the pharmaceutical industry, it is widely applied as an excipient for drugs (Liew et al., 2006), a dental impression material (Ashley et al., 2005), and a wound dressing (Matthew et al., 1995).

As a biomaterial, alginate possesses many advantageous features such as biocompatibility and nonimmunogenicity. They are possibly because of its hydrophilicity (Shapiro and Cohen, 1997). A significant advantage is its easy gelling behavior, which induces entrapping of various substances with minimum trauma (Klock et al., 1997). A chemically modified alginate is currently used clinically as a drug delivery vehicle for proteins that promote regeneration of mineralized tissue (Bratthall et al., 2001) and as a carrier for transplanted cells (Bent et al., 2001). One of its disadvantages is that enzymes cannot naturally break it down in mammals and hence has poorly controlled degradation (Lansdown and Payne, 1994). In addition to those, cells do not naturally adhere to alginate (Smetana Jr, 1993). There has been impressive research over the past decade to handle these problems and to widen the utility of alginate hydrogels (Augst et al., 2006).

1.1.4.2 Chitosan

Chitosan is a positively-charged polysaccharide that is extracted from chitin which is the main structural polymer in arthropod exoskeletons (Muzzarelli, 1977, Muzzarelli et al., 1986). Since its molecular weight is relatively high, between 300-1000 kDa, depending on the source of chitin and extraction method, applications composed of this polymer have high tensile modulus and thus can be used in a wide array of application (Dvir et al., 2005).

Chitin is the second most abundant polysaccharide in nature, exceeded only by cellulose. This renewable resource is found in numerous naturally occurring organisms such as fungi, yeast, algae and is the principal component in the exoskeleton of sea crustaceans (Figure 1.7), such as shrimp and crab as well as in the cuticle and ovipositors of insects (Hudson and Jenkins, 2002).

Figure 1. 7 Crustaceans

Chitin possesses a homogeneous chemical composition composed of 1-4 linked 2-acetamido-2-deoxy-β-D-glucopyranose (Figure 1.8).

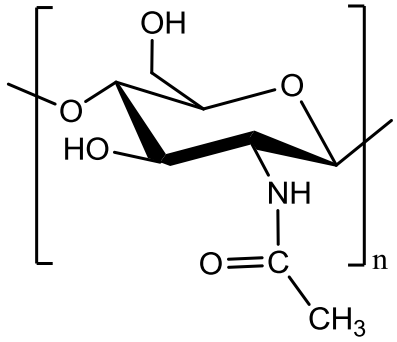

Figure 1. 8 Chemical structure of chitin

While chitin is naturally available in great amounts through many sources, chitosan is only accessible in nature in limited quantities, such as in some fungi: mucor rouxi, aspergillis nidulans (Hudson and Jenkins, 2002). The chitosan used in industrial and research applications is generally extracted from chitin by the use of chemical or enzymatic treatments of the shells of Arthropoda (shrimp or crab) secured from the waste products of the crabbing and shrimping industries. Several chemical, mechanical, and enzymatic methods have been developed to acquire purified chitosan. The common method to extract chitosan is the chemical treatment of shell fish wastes from the crab and shrimp industries. First, the shell is demineralized in dilute hydrochloric acid at room temperature. Second, it is deprotenized in warm dilute caustic. This forms a partially deacetylated chitin which finally is further deacetylated to chitosan. Through deacetylation process of chitin, chitosan with 70% to 95% deacetylation degree is obtained (Hudson and Jenkins, 2002).

Chitosan, a partially deacetylated derivative of chitin, has at least 50% of the free amine groups. Therefore, it has a varying chemical structure consisting of both 1-4

linked 2-acetamido-2-deoxy-β-D-glucopyranose as well as 2-amino-2-deoxy-β-D-glucopyranose (Figure 1.9).

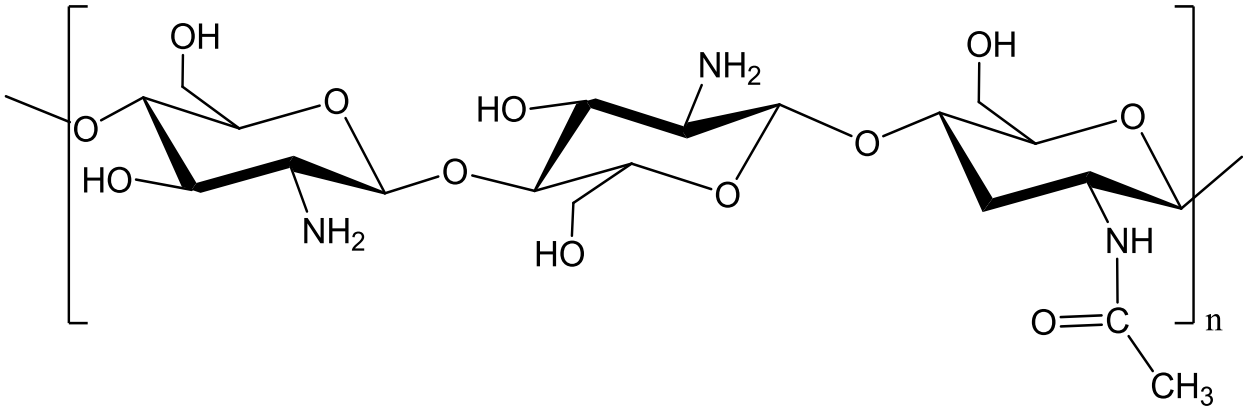

Figure 1. 9 Chemical structure chitosan

As the process conditions control the extent of deacetylation that occurs, the properties of chitosan are mainly affected by the conditions under which it is processed. The degree of deacetylation (DD) sets the amount of free amino groups in the polymer backbone. The free amino groups provide the positive charge to chitosan. The functionality of chitosan which allows it to be a highly reactive polysaccharide is provided by the amino group and the hydroxyl groups together. The positive charge of chitosan enables it to make a great number of electrostatic interactions with negatively charged molecules. The extent of functional groups generated by deacetylation and the processing conditions support side group attachment, which then affects crystallinity that directly links to chitosan's ability to solubilize in acidic aqueous solutions, an important phenomena of the processability of chitosan (Hudson and Jenkins, 2002, Sßenel and McClureb, 2004).

Some biological properties including biodegradability, lack of toxicity, anti-fungal effects, wound healing acceleration, and immune system stimulation of chitosan make it promising material for the needs in medical applications (Di Martino et al., 2005, Hudson and Jenkins, 2002, Khor and Lim, 2003, Sßenel and McClureb, 2004). The biological and chemical properties of chitosan provide the potential to make bonds with particular materials such as cholesterols, fats, proteins, metal ions, and even tumor cells. Thus enables chitosan to be utilized as a chelating agent in many applications (Li et al., 1992).

The degradation of chitosan can be accomplished through several methods. Owing to its degradation rate that is inversely proportional to the degree of crystallinity and consequently the amount of deacetylation, degradation can be engineered by controlling the amount of deacetylation that takes place during processing. Chitosan can be thermally degraded at temperatures above 280^{o}C and also polymer chains decompose fast. Enzymatic degradation is an important means of handling the decomposition of chitosan. A wide range of hydrolytic enzymes, such as lysozyme (the primary enzyme responsible for degradation of chitosan), encountered in the lyphoid systems of humans and animals, can be exerted to naturally degrade chitosan (Di Martino et al., 2005, Hudson and Jenkins, 2002). The degradation of chitosan within the body leads to the release of amino-sugars which can be easily processed and metabolize through the organic system. Degradation is a substantial property to comprehend so that the processing and the end applications can be engineered accordingly (Sßenel and McClureb, 2004).

Due to chitosan's many attractive properties such as biodegradability, natural origin, abundance, reactivity, it has many areas of application including: medical, agricultural, food processing, nutritional enhancement, cosmetics, and waste and water treatment (Hudson and Jenkins, 2002, Sßenel and McClureb, 2004).

The biodegradability, profusion, lack of toxicity, and natural origin of chitosan make it used reliably in agricultural applications without concerns of pollution, discarding, or negative effect to consumers if eaten (Li et al., 1992). Some of the applications within agricultural use are seed coating, leaf coating, fertilizer, and time released drug or fertilizer responses where chitosan has found utility (Li et al., 1992). The applications in these areas include raising the harvest by enhancing germination, rooting, leaf growth, seed yield, and soil moisture retention, while decreasing the occurrence of fungal infections and diseases (Li et al., 1992).

The functional groups and natural chelating properties of chitosan are utilized extensively in wastewater treatment by inducing for the binding and removal of metal ions such as copper, lead, mercury, and uranium from wastewater (Hudson and Jenkins, 2002). The breakdown of food particles that contain protein and removal of dyes and other negatively charged solids from wastewater streams and processing outlets are the other applications for chitosan (Li et al., 1992).

Several valuable applications within the food industry such as binding with and removing certain elements, particles, and materials such as dyes and fats from foods come from its chelating properties and high functionality (Li et al., 1992). The antimicrobial and antifungal properties occurring in chitosan make it efficient during the storage and preservation of food (Hudson and Jenkins, 2002, Li et al., 1992).

Because chitosan functions in numerous shapes, there is a great deal of use and interest within the medical industry for uses such as drug delivery, wound healing, orthopedic, periodontal, and tissue engineering (Khor and Lim, 2003). It has been greatly modified and used for drug delivery systems in oral, parenteral, transdermal, ocular, and nasal applications especially due to its low toxicity with outstanding mucoadhesion properties (Paul and Sharma, 2000). Chitosan gels and films displayed sustained release of different drugs efficient for wound dressings and colon treatments (Hudson and Jenkins, 2002). Wound dressing of chitosan can stimulate some various physiological activities (Muzzarelli, 1997). On the wound surface, they induce macrophage activity to discharge lysozyme and human chitinase, enzymes which separates chitin-based pathogens to prevent infection (Hudson and Jenkins, 2002). Because of chitosan's excellent fiber and film forming ability, it has been blended with other polymers to control permeability and to improve blood compatibility in membrane applications for hemodialysis patients (Rathke and Hudson, 1994).

1.2 RESEARCH OBJECTIVES

There are two main objectives associated with this research:

The first objective of this work is to understand and evaluate the problems associated with the composition of chitosan and alginate. Different forms of the composition will be evaluated and its quality will be assessed as possible biomaterial applications for different areas.

The second objective is to obtain a basic understanding of the thermal, mechanical, morphological, and antibacterial properties of the each component as well as their compositions.

REFERENCES

ASHLEY, M., MCCULLAGH, A. & SWEET, C. 2005. Making a good impression:(a'how to'paper on dental alginate). *Dental update,* 32**,** 169.

AUGST, A. D., KONG, H. J. & MOONEY, D. J. 2006. Alginate hydrogels as biomaterials. *Macromolecular bioscience,* 6**,** 623-633.

BENT, A. E., TUTRONE, R. T., MCLENNAN, M. T., LLOYD, K., KENNELLY, M. J. & BADLANI, G. 2001. Treatment of intrinsic sphincter deficiency using autologous ear chondrocytes as a bulking agent. *Neurourology and Urodynamics,* 20**,** 157-165.

BRATTHALL, G., LINDBERG, P., HAVEMOSE POULSEN, A., HOLMSTRUP, P., BAY, L., SÖDERHOLM, G., NORDERYD, O., ANDERSSON, B., RICKARDSSON, B. & HALLSTRÖM, H. 2001. Comparison of ready to use EMDOGAIN® gel and EMDOGAIN® in patients with chronic adult periodontitis. *Journal of Clinical Periodontology,* 28**,** 923-929.

CAIRNS, P., MILES, M. J., MORRIS, V. J. & BROWNSEY, G. J. 1987. X-ray fibre-diffraction studies of synergistic, binary polysaccharide gels. *Carbohydrate research,* 160**,** 411-423.

CHATTERJEE, S. K., GUPTA, S. & SETHI, K. R. 1987. Study of CU(II)-methacrylic acid — methacrylamide copolymer interactions and formation of metal-copolymer complexes. *Die Angewandte Makromolekulare Chemie,* 147**,** 133-146.

CIMA, F., BALLARIN, L., BRESSA, G., MARTINUCCI, G. & BURIGHEL, P. 1996. Toxicity of organotin compounds on embryos of a marine invertebrate (Styela plicata; Tunicata). *Ecotoxicology and environmental safety,* 35**,** 174-182.

CLARK, A., RICHARDSON, R., ROSS-MURPHY, S. & STUBBS, J. 1983. Structural and mechanical properties of agar/gelatin co-gels. Small-deformation studies. *Macromolecules,* 16**,** 1367-1374.

D'AYALA, G. G., MALINCONICO, M. & LAURIENZO, P. 2008. Marine derived polysaccharides for biomedical applications: Chemical modification approaches. *Molecules,* 13**,** 2069-2106.

DI MARTINO, A., SITTINGER, M. & RISBUD, M. V. 2005. Chitosan: a versatile biopolymer for orthopaedic tissue-engineering. *Biomaterials,* 26**,** 5983-5990.

DRAGET, K., PHILLIPS, G. & WILLIAMS, P. 2009. Alginates. *Handbook of hydrocolloids***,** 807-828.

DRAGET, K., SMIDSROD, O. & SKJAK-BRAK, G. 2005. Alginates from algae. Polysaccharides and polyamides in the food industry. Properties, production, and patents. Steinbüchel A, Rhee SK (Editores).

DUMITRIU, S. 2002. Polysaccharides as biomaterials. *Polymeric biomaterials***,** 1–61.

DUPUY, B., ARIEN, A. & MINNOT, A. P. 1994. FT-IR of membranes made with alginate/polylysine complexes. Variations with the mannuronic or guluronic content of the polysaccharides. *Artificial Cells, Blood Substitutes and Biotechnology,* 22**,** 71-82.

DURRANI, C. M. & DONALD, A. M. 1994. Fourier transform infrared microspectroscopy of phase-separated mixed biopolymer gels. *Macromolecules,* 27**,** 110-119.

DVIR, T., TSUR GANG, O. & COHEN, S. 2005. “Designer” scaffolds for tissue engineering and regeneration. *Israel journal of chemistry,* 45**,** 487-494.

EHRLICH, H., KRAUTTER, M., HANKE, T., SIMON, P., KNIEB, C., HEINEMANN, S. & WORCH, H. 2007. First evidence of the presence of chitin in skeletons of marine sponges. Part II. Glass sponges (Hexactinellida: Porifera). *Journal of Experimental Zoology Part B: Molecular and Developmental Evolution,* 308**,** 473-483.

GEORGE, M. & ABRAHAM, T. E. 2006. Polyionic hydrocolloids for the intestinal delivery of protein drugs: alginate and chitosan--a review. *Journal of Controlled Release,* 114**,** 1-14.

GLICKSMAN, M. 1987. Utilization of seaweed hydrocolloids in the food industry. *Hydrobiologia,* 151-152**,** 31-47.

HAUG, A. 1964. *Composition and properties of alginates.* Thesis, Norwegian Institute of Seaweed Research, Trondheim.

HAUG, A. & LARSEN, B. 1962. Quantitative determination of the uronic acid composition of alginates. *Acta Chem. Scand,* 16**,** 1908-1918.

HAUG, A., LARSEN, B. & SMIDSROD, O. 1967. Studies on the sequence of uronic acid residues in alginic acid. *Acta Chem. Scand,* 21**,** 691-704.

HUDSON, S. M. & JENKINS, D. W. 2002. Chitin and chitosan. *Encyclopedia of Polymer Science and Technology.* John Wiley & Sons, Inc.

INDERGAARD, M. & SKJÅK-BRÆK, G. 1987. Characteristics of alginate from Laminaria digitata cultivated in a high-phosphate environment. *Hydrobiologia,* 151**,** 541-549.

KHOR, E. & LIM, L. Y. 2003. Implantable applications of chitin and chitosan. *Biomaterials,* 24**,** 2339-2349.

KLOCK, G., PFEFFERMANN, A., RYSER, C., GROHN, P., KUTTLER, B., HAHN, H. J. & ZIMMERMANN, U. 1997. Biocompatibility of mannuronic acid-rich alginates. *Biomaterials,* 18**,** 707-713.

KRISHNAN, G. 1975. Nature of tunicin & its interaction with other chemical components of the tunic of the ascidian, Polyclinum madrasensis Sebastian.

KUBOTA, N. & KIKUCHI, Y. 1998. Macromolecular complexes of chitosan. *Polysaccharides: Structural diversity and functional versatility. Marcel Dekker Inc., USA*.

LANSDOWN, A. & PAYNE, M. 1994. An evaluation of the local reaction and biodegradation of calcium sodium alginate (Kaltostat) following subcutaneous implantation in the rat. *Journal of the Royal College of Surgeons of Edinburgh,* 39**,** 284.

LI, Q., DUNN, E., GRANDMAISON, E. & GOOSEN, M. 1992. Applications and properties of chitosan. *Journal of bioactive and compatible polymers,* 7**,** 370.

LIEW, C. V., CHAN, L. W., CHING, A. L. & HENG, P. W. S. 2006. Evaluation of sodium alginate as drug release modifier in matrix tablets. *International Journal of Pharmaceutics,* 309**,** 25-37.

MATTHEW, I. R., BROWNE, R. M., FRAME, J. W. & MILLAR, B. G. 1995. Subperiosteal behaviour of alginate and cellulose wound dressing materials. *Biomaterials,* 16**,** 275-278.

MCLACHLAN, J. 1985. Macroalgae (seaweeds): industrial resources and their utilization. *Plant and Soil,* 89**,** 137-157.

MORRIS, E. R., REES, D. A. & THOM, D. 1973. Characterization of polysaccharide structure and interactions by circular dichroism: order–disorder transition in the calcium alginate system. *J. Chem. Soc., Chem. Commun.***,** 245-246.

MORRIS, V. 1998. Gelation of polysaccharides. *Functional properties of food macromolecules***,** 143.

MUZZARELLI, R. 1997. Human enzymatic activities related to the therapeutic administration of chitin derivatives. *Cellular and molecular life sciences,* 53**,** 131-140.

MUZZARELLI, R. A. A. 1977. *Chitin,* Oxford, Pergamon.

MUZZARELLI, R. A. A., JEUNIAUX, C. & GOODAY, G. W. 1986. *Chitin in nature and technology*, Plenum Pub Corp.

PAUL, W. & SHARMA, C. 2000. Chitosan, a drug carrier for the 21st century: a review. *STP pharma sciences,* 10**,** 5-22.

RATHKE, T. D. & HUDSON, S. M. 1994. Review of chitin and chitosan as fiber and film formers. *Polymer Reviews,* 34**,** 375-437.

REES, D. A. & WELSH, E. J. 1977. Secondary and Tertiary Structure of Polysaccharides in Solutions and Gels. *Angewandte Chemie International Edition in English,* 16**,** 214-224.

SCRANTON, A., KLIER, J. & ARONSON, C. 1992. Complexation of polymeric acids with polymeric bases. 1992. ACS Publications, 171-189.

SHAPIRO, L. & COHEN, S. 1997. Novel alginate sponges for cell culture and transplantation. *Biomaterials,* 18**,** 583-590.

SIME, W. 1990. Alginates. *Food Gels***,** 53-78.

SMETANA JR, K. 1993. Cell biology of hydrogels. *Biomaterials,* 14**,** 1046-1050.

SMIDSRØD, O. & SKJAOK-BRK, G. 1990. Alginate as immobilization matrix for cells. *Trends in Biotechnology,* 8**,** 71-78.

SßENEL, S. & MCCLUREB, S. J. 2004. Potential applications of chitosan in veterinary medicine. *Advanced drug delivery reviews,* 56**,** 1467-1480.

SUTHERLAND, I. 1991. Alginates In Biomaterials, novel materials from biological sources, D. *Stockton ress. New York, NY***,** 307-331.

TAKAYANAGI, M., HARIMA, H. & IWATA, Y. 1963. Viscoelastic behavior of polymer blends and its comparison with model experiments. *Mem. Fac. Eng. Kyushu Univ,* 23**,** 1-13.

TSUCHIDA, E., ABE, K. & SPRINGERLINK 1982. *Interactions between macromolecules in solution and intermacromolecular complexes*, Springer-Verlag Berlin.

CHAPTER TWO

CHARACTERIZATION OF CHITOSAN-ALGINATE FILMS

2.1 INTRODUCTION

Recently, the growing interest in the development and the application of new materials from renewable sources shows a trend away from synthetic polymers and towards natural polymers in different areas such as food science, medicine, and cosmetics (Neto et al., 2005). This tendency has certainly occurred in food packaging due to the growing public health concern, the reducing environmental impact, safety, and convenience (Pereda et al., 2008). The biodegradability and biocompatibility are the main functional advantages of natural polymers in food packaging. An advantageous fact of the biodegradable packaging materials is that through biodegradation and decomposition, they could be also used in secondary applications such as fertilizer or soil conditioner, providing a better harvest. Even though it is slightly expensive, biodegradable packaging is the premise of user friendly and eco-friendly packaging (Srinivasa and Tharanathan, 2007).

Among various food packaging materials, polysaccharide based films have drawn considerable attention. Different types of polysaccharides and their derivatives have been utilized as biodegradable film-forming matrixes (Rhim and Ng, 2007). Along the process of polysaccharide film formation, the separation of polymer segments and

reorganization of the polymer chain into a film matrix or gel occur through the evaporation of a solvent that generates hydrophilic and hydrogen bonding (Rhim and Ng, 2007).

Chitosan, one of the commonly used polysaccharides, is a cationic biopolymer that has unique nutritional, biomedical, and functional properties (Takahashi et al., 1990, Pereda et al., 2008). It has been used in many application areas, such as agriculture, waste water treatment, food industry, and biomedicine. The commercially available form of chitosan is mostly the deacetylated chitin, which is the second abundant polysaccharide on earth after cellulose and is extracted from waste products of the shellfish industry (Xu et al., 2005).

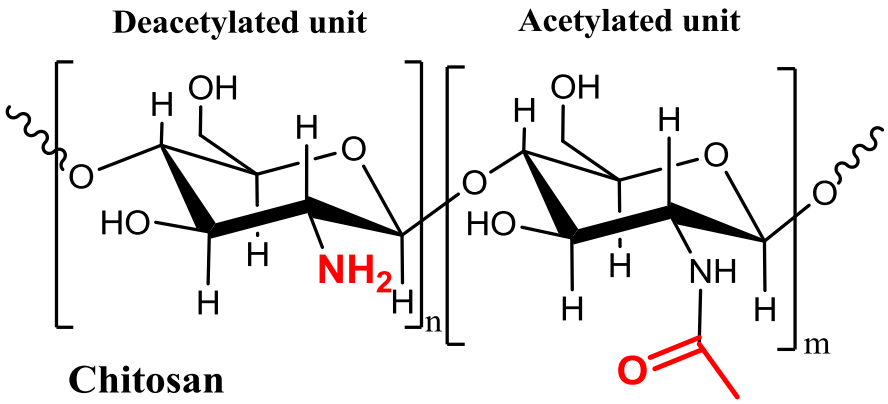

Figure 2. 1 Structure of chitosan

Unlike chitin, there are reactive amino and hydroxyl groups on chitosan backbone that can be used for chemical reactions and salt formation (Figure 2.1). These groups, due to their hydrophilicity, have an important impact on permeability and diffusion of water through chitosan films (Meng et al., 2009). From earlier studies,

chitosan has been recognized to carry effective film forming properties, chemical resistance, and high permselectivity for water (Meng et al., 2009). The neutralization of -NH_3^+ sites into -NH_2 in chitosan caused to the vanishing of the ionic repulsions between polymer chains; therefore, physically cross-linked formation related to hydrogen bonding, hydrophobic interactions and crystallite formation were preferred (Meng et al., 2009). This property has been applied on edible films by forming electrostatic interactions with anionic groups in an acid environment (Xu et al., 2005).

Alginate is the main structural component in marine brown algae. The intercellular alginate gel matrix provides plants both tenacity and resilience (Draget et al., 2009). It is known as potential biopolymer film or coating material because it has unique and well examined colloidal properties, such as thickening, stabilizing, suspending, and film and gel forming properties (Zactiti and Kieckbusch, 2006). It has been widely used in industry including uses in agriculture, medicine, pharmacy, food processing, and construction. As extracted from brown algae, alginate is a water-soluble linear polysaccharide and consists of alternating blocks of 1–4 linked α-L-guluronic (G) and β-D-mannuronic (M) acid residues (Figure 2.2) (George and Abraham, 2006). The order and the chemical configuration of the M and G blocks are dependent on the biological source, growth and seasonal conditions (George and Abraham, 2006).

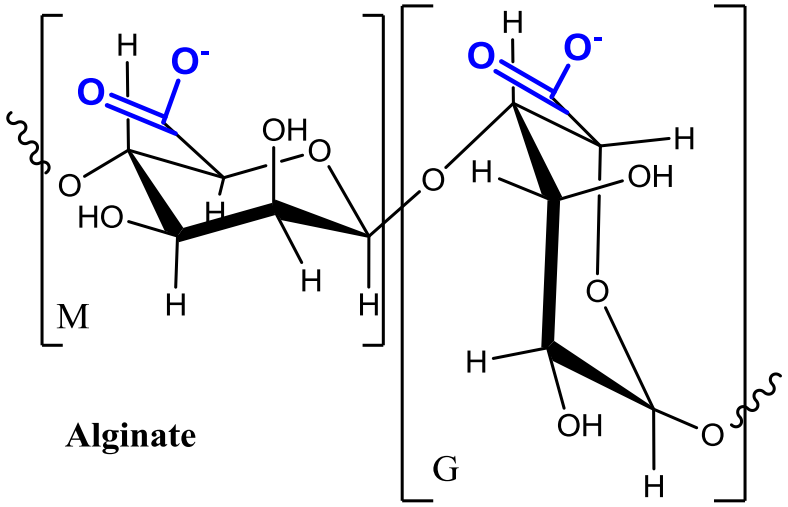

Figure 2. 2 Structure of alginate

Several studies on chitosan based films have been reported, such as chitosan-starch (Lazaridou and Biliaderis, 2002, Xu et al., 2005, Zhai et al., 2004), chitosan-pullulan (Lazaridou and Biliaderis, 2002), chitosan-gelatin (Arvanitoyannis et al., 1998, Chatterjee et al., 1987, Kolodziejska and Piotrowska, 2007), chitosan-PVA (Arvanitoyannis et al., 1997), and chitosan-amylose starch (Cervera et al., 2004). However, according to our literature review, studies on chitosan-alginate films are rarely found. By processing these films, advantages might be found from the electrostatic interactions through the $-NH_3^+$ groups of chitosan, as a cationic polymer, with anionic groups, such as $-COO^-$ groups, present in alginate or polyanions (Pereda et al., 2008). These interactions illustrated in Figure 2.3 play an important role in the formation of polymeric complexes (Pereda et al., 2008).

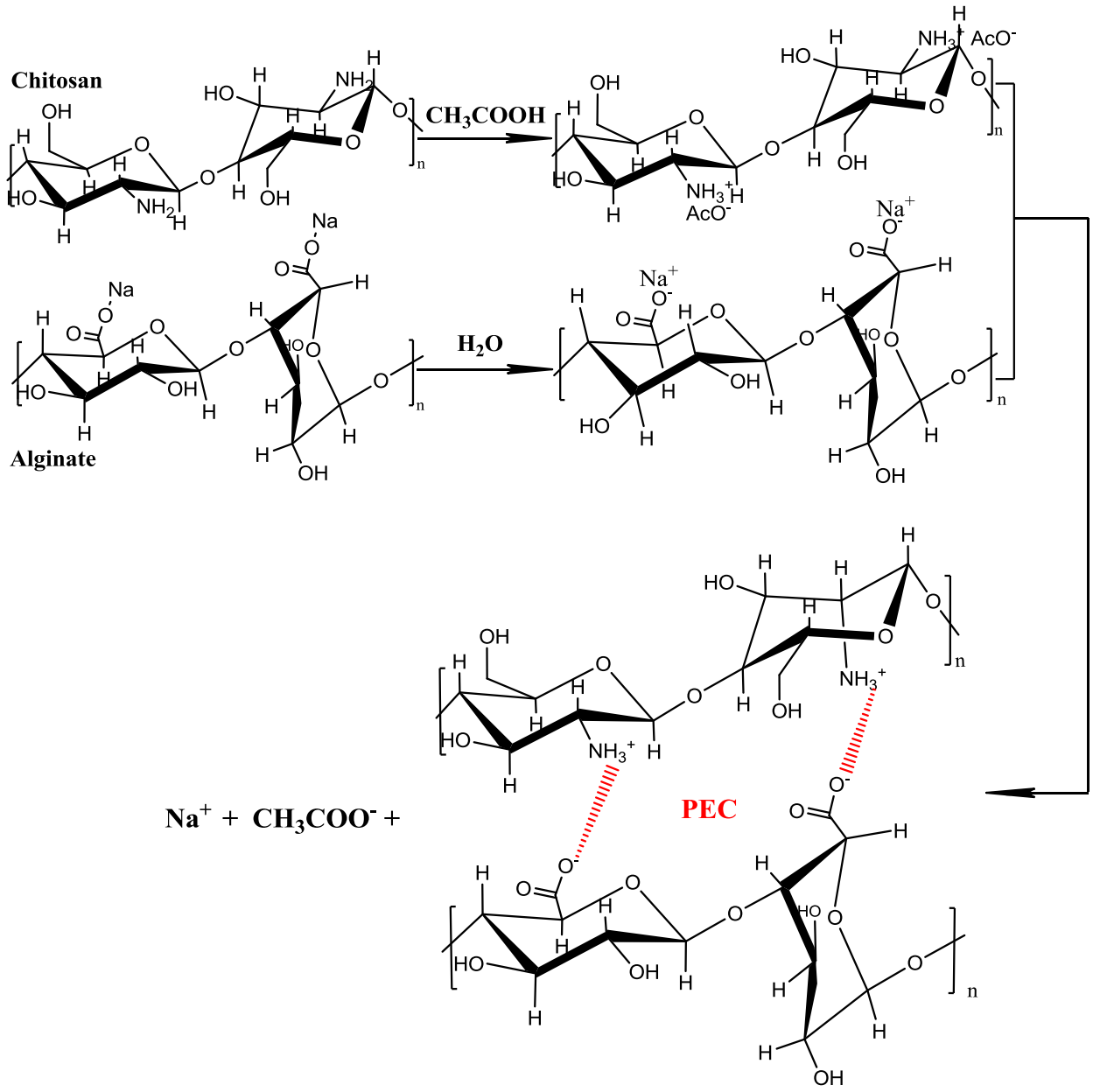

Figure 2. 3 Structural scheme of chitosan–sodium alginate ion complex formation reaction between anion group (–COO^-) of sodium alginate and the protonated cation group (–NH_3^+) of chitosan

Chitosan and sodium alginate are both natural polymers, and both have biocompatibility, biodegradability, and hydrophilicity. Therefore, chitosan-sodium alginate polymer mixtures have the potential to produce new functional polymers with

good performance, which can be used in various applications. In this chapter, chitosan-alginate polymer films were prepared and miscibility, thermal stability, mechanical morphological properties of the films were studied by infrared (FTIR) spectra, scanning electron microscopy (SEM), thermogravimetric analyzer (TGA), differential scanning calorimeter (DSC) and dynamic mechanical analyzer (DMA). In addition to these analyses, antibacterial properties of the films were tested through zone inhibition test.

2.2 EXPERIMENTAL

2.2.1 Materials

Commercial medium molecular weight (MMW) chitosan (average molecular weight (Mw) = 400,000 Da and deacetylation degree (DD) 80%) was supplied by Sigma-Aldrich Corp., St. Louis, MO. Commercial sodium alginate and glacial acetic acid (CH_3COOH) were purchased from Fisher Scientific, Pittsburgh, PA. For nuclear magnetic resonance test, deuterated acetic acid (CD_3COOD) and deuterium oxide (D_2O) were also purchased from Fisher Scientific. For zeta potential measurements, sodium hydroxide (NaOH) and hydrochloric acid (HCl) were purchased from Sigma-Aldrich Corp., St. Louis, MO.

2.2.2 Methods and Techniques

2.2.2.1 Nuclear magnetic resonance (NMR) spectroscopy

The molecular structure and properties of chitosan is extensively dependent upon the degree of deacetylation (Hirai et al., 1991). As a result, it was essential to determine precisely the degree of deacetylation. For this determination, two methods have been reported in literature besides NMR spectroscopy: (i) Colloid titration

evaluating amino residue (Terayama, 1952), and (ii) Elemental analysis and transmission ratio of infrared spectrum evaluating carbon/nitrogen ratio (Miya et al., 1980, Sannan et al., 1978). The effect of high moisture absorbency of chitosan cannot be completely removed with these methods above and also a great amount of sample is to be consumed in the case of colloid titration; therefore, ^{1}H NMR spectroscopy is selected. In ^{1}H NMR, small amount of sample (~5mg) is needed and water sorption can be eliminated (Hirai et al., 1991).

^{1}H NMR spectra of chitosan was performed on a Bruker AV-400 spectrometer, operating at 400 MHz. Medium molecular weight chitosan was dissolved in 2 wt% CD_3COOD/D_2O solution at room conditions. After dissolution, approximately 1 ml of the chitosan solution was transferred to a 5 mm NMR tube. The sample tube was inserted in the magnet and allowed to reach thermal equilibrium by waiting 10 minutes before performing the experiment. Integration boundaries of obtained spectrum were adjusted manually by the analyst's judgment. ^{1}H chemical shifts were expressed in ppm downfield from the signal for sodium 3-(trimethylsilyl) propane sulfonate (TSP) as an external reference.

2.2.2.2 Zeta (ζ) potential measurements

Zeta potential measurements of chitosan, alginate and their mixture solutions were performed with a Particle Sizer Analyzer NICOMP at 25ºC. Measurements were performed as a function of pH in buffered solutions. The measurements were carried out in triplicate. All the values were measured with a relative accuracy of 1%.

2.2.2.3 Film preparation

Solution casting is the chosen method for the preparation of films. Chitosan solutions (1% w/v) were prepared by adding chitosan powder in acetic acid solution (1% v/v). Sodium alginate solution (1% w/v) was prepared by dissolving alginate powder in distilled water. Both solutions were filtered through a 325 mesh stainless steel woven disk filter.

Different proportions of chitosan and sodium alginate solutions (100:0, 20:80, 40:60, 50:50, 60:40, 80:20, 0:100 CH:AL) were prepared by manual stirring, then poured into glass Petri dishes (Ø = 9 cm) and finally kept in the laboratory condition (21°C, 50% RH) for 24 hours to remove air bubbles. After that the films were dried at constant temperature (30°C) overnight in a convection oven, resulting in films with thicknesses between 45 and 55 µm. After the drying stage, the films were peeled off from the glass plates and kept in a desiccator at ambient conditions.

Table 2. 1 Chitosan-alginate film compositions

	Volume (ml)	
Chitosan-Alginate (CH:AL) (%)	**Chitosan (1.0 % w/v)**	**Alginate (1.0 % w/v)**
100:0	40	0
80:20	32	8
60:40	24	16
50:50	20	20
40:60	16	24
20:80	8	32
0:100	0	40

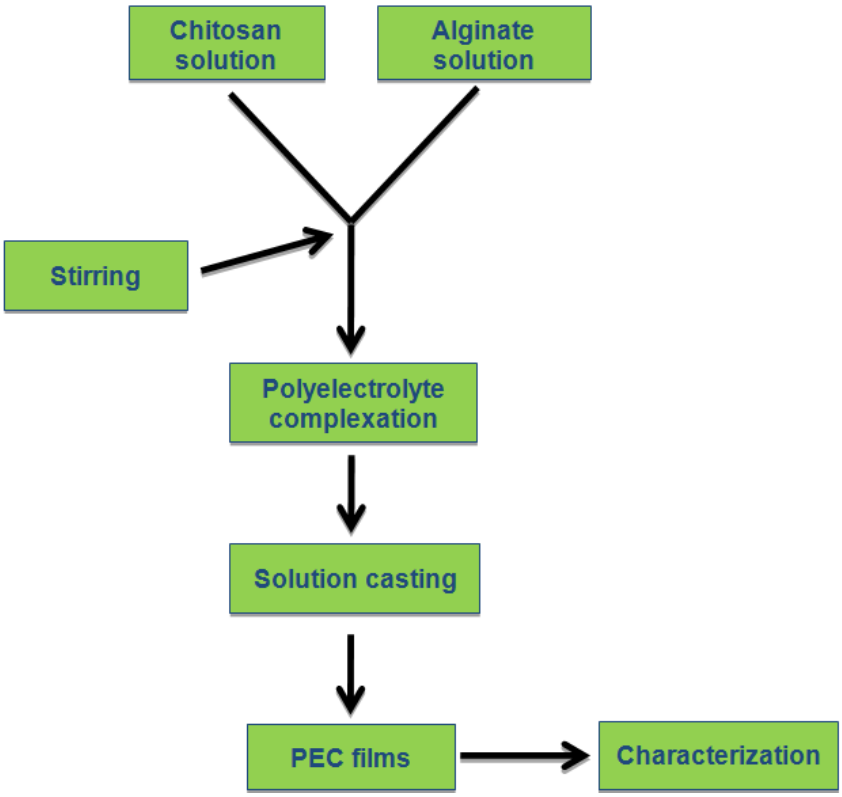

Figure 2. 4 Illustration of film preparation process

2.2.2.4 Light transmission properties

Light transmission tests were performed in a UV-VIS Spectrophotometer (UV-2450 Shimadzu Scientific) under wavelength 400~750 nm. Each dry film (3cm×1cm) was fixed onto the wall of the sample holder. Film transparency was determined by measuring the amount of light transmitted through the films relative to air.

2.2.2.5 Infrared spectroscopy characterization

Infrared spectrums of the films were measured by attenuated total reflection method (ATR) using a Thermo Nicolet 6700 Fourier transform infrared spectrometer connected to a PC with OMNIC software analysis. The thickness of the films used was

about 45-55 µm. All spectrums were recorded between 400 and 4000 cm^{-1} over 32 scans with a resolution of 4 cm^{-1}.

2.2.2.6 Thermogravimetric analysis (TGA)

TGA thermograms of the films were measured on a Thermogravimetric Analysis (TA) Instrument Q500. All analyses were carried out with ~5 mg samples in platinum pans under a dynamic nitrogen atmosphere between 25–500°C at a heating rate of 10°C/min under nitrogen purge.

2.2.2.7 Differential scanning calorimetry (DSC)

Differential scanning calorimetric test was performed using a Differential Scanning Calorimeter TA Instruments DSC 2920. Samples (~5 mg) were placed in aluminum pans with lids. The test included two runs; first run from -50 to 180°C and the second one from -50 to 280°C with a scanning rate of 10°C/min.

2.2.2.8 Dynamical mechanical analysis (DMA)

DMA measurements were performed on a Dynamic Mechanical Analyzer (DMA RSA3 TA Instruments) at 1 Hz and a heating rate of 2°C/min. DMA curves were obtained in two cycles of heating run: the first one of heating up to 110°C then holding there for 10 minutes followed by cooling to 30°C and the second one of heating up to 250°C. The samples were cut 20.0 mm long, 5 mm wide and about 0.04 mm thick. The samples were not clamped during the first heating and subsequent cooling process in order to avoid residual stress.

2.2.2.9 Scanning electronic microscopy analyses

The fractured surfaces of films pre-chilled in liquid nitrogen were studied by scanning electron microscope (SEM, Cambridge 360). Samples were sputtered with gold prior to SEM observation.

2.2.2.10 Mechanical properties

During this research, tensile tests were performed in order to evaluate the mechanical response of films.

Tensile tests: Film thicknesses were measured using a 0–25 mm automatic micrometer, with a resolution of 0.01 mm. The reported values are the average of 10 readings taken randomly on each film sample. Tensile tests were performed according to the ASTM D1708-93 (1993) with a Dynamic Mechanical Analyzer (DMA RSA3 TA Instruments) in multiple extension mode at room temperature (23°C ± 2°C). A film strip (dimensions 2.0 cm×0.5 cm) was clamped between grips and stretched by top grip at rate of 0.05 mm/sec. The yield strength (σ_y), elongation at break (ε_b) and elastic modulus (*E*) were calculated as described in ASTM D638-94b (1994).

2.2.2.11 Antibacterial testing - Zone of inhibition test

In vitro antibacterial behavior of the 100:0, 60:40, 80:20, 0:100 CH:AL films were evaluated by inhibition zone experiments against Gram-negative bacterium (*Escherichia coli)*. The films were cut into 2x2 cm^2 and then placed on nutrient agar plates coated with the bacteria with a concentration of approximately 10^5 CFU/ml. Finally, the plates were incubated at 37°C for 24 hours, and the inhibition zone was measured.

2.3 RESULT AND DISCUSSION

2.3.1 NMR study for the determination of the degree of deacetylation

The ^{1}H-NMR spectrum of chitosan is shown in Figure 2.5. HOD band appeared due to dissolution of chitosan in 2 wt% CD_3COOD/D_2O and its proton which is not bonded to chitosan resonates at 4.62 ppm. All other chemical shifts of chitosan protons, also similarly reported by Hirai et al. (1991) and Varum et al. (1991), are shown in Table 2.2.

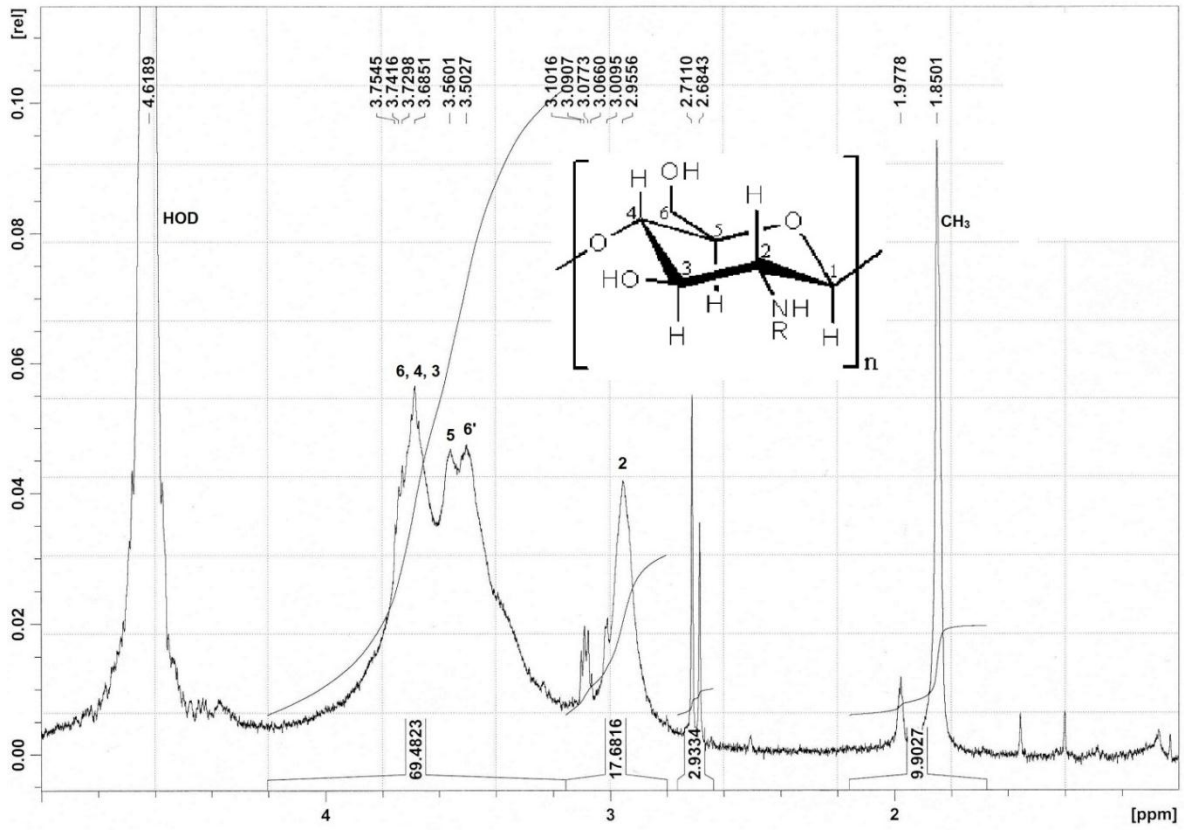

Figure 2. 5 ^{1}H NMR spectrum of chitosan (DD = 80%), in CD_3COOD/D_2O, at 400 MHz

Table 2. 2 Chitosan chemical shifts of proton at room conditions in CD_3COOD/D_2O

Proton	Chemical Shift (ppm)
H_1	5.36
H_2	2.95
$H_{3, 4, 5, 6, 6'}$	3.73, 3.69, 3.56, 3.5
N-acetyl	1.85

Deacetylation degree (DD) of chitosan is calculated from Equation (1) (Hirai et al., 1991) by using the integral intensity, I_{CH_3}, of this CH_3 residue, and the total of integral intensities, $I_{H_2-H_6}$, of H_2, H_3, H_4, H_5, H_6, and $H_{6'}$ protons.

$$DD\ (\%) = \left[1 - \left(\frac{1}{3} I_{CH_3} / \frac{1}{6} I_{H_2-H_6}\right)\right] * 100 \qquad \text{Equation (1)}$$

Through the NMR spectra of chitosan ($I_{CH_3} = 9.9027$, $I_{H_2-H_6} = 51.8007$) the deacetylation degree (DD) was calculated 79% which is almost the same degree as the provider's claim, ~80%.

2.3.2 Zeta (ζ) potential measurements

Zeta potential of 0.1 w/v% chitosan and 0.1 w/v% alginate solutions and their mixture of 50:50 with the same concentrations were measured with 0.1 pH unit of a chosen value with 0.1 or 1 M NaOH or HCl solution. The results are shown in Figure 2.6.

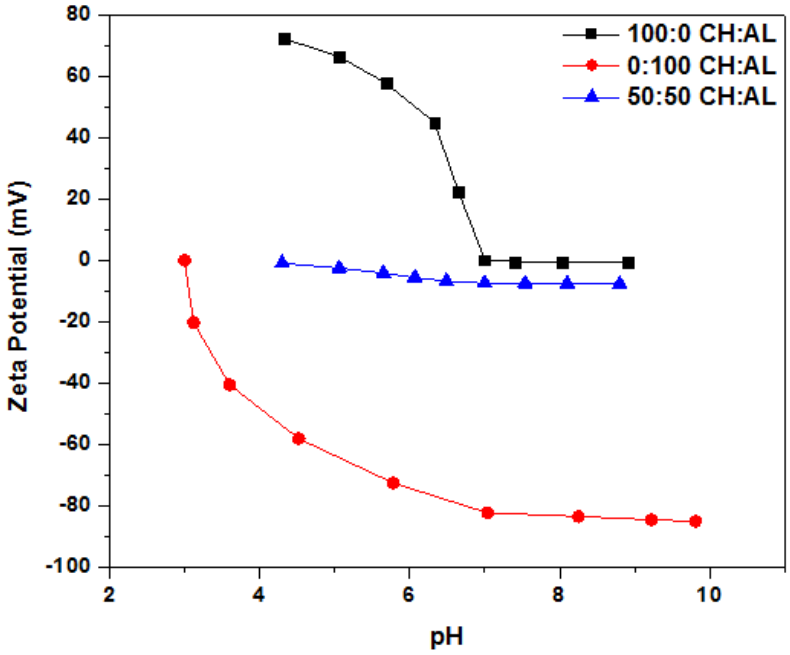

Figure 2. 6 Zeta potential of the solutions of chitosan, alginate and their mixture

Chitosan begins precipitating above pH 6.6 and its zeta potential declines to zero at pH 7±0.1 which is its isoelectric point indicating no net charge. Below its precipitation point, chitosan has high positive zeta potential confirming the cationicity of the polymer. However, alginate dissolved in water carries negative charge at pH 7±0.1. Below that point, the net charge of alginate solution decreases and reaches zero at pH 3.0±0.1. The 50:50 solution of chitosan and alginate has a negative charge above pH 4.3 indicating the excess negative charge on account of alginate. In acidic medium, the mixture solution carries almost no net charge which most likely occurred due to electrostatic interaction between cationic chitosan and anionic alginate.

2.3.3 Light transmission properties

The transparency of prepared samples is reported in Figure 2.7. The light transmission of all the films increases with the wavelength.

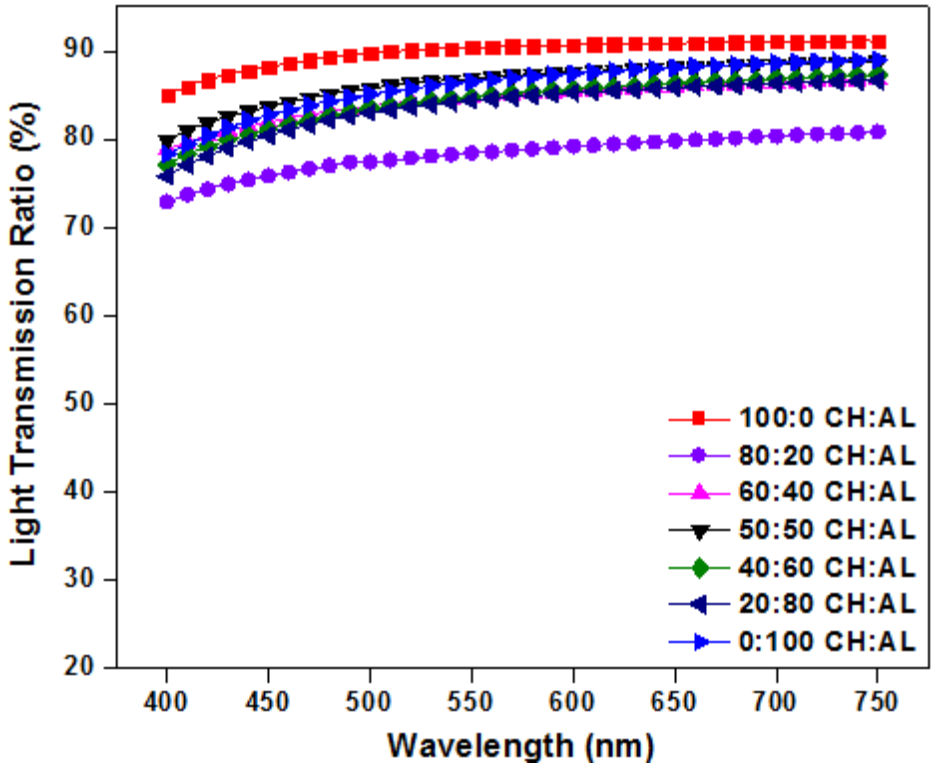

Figure 2. 7 Light transmission of different composition of films

In the range of visible light spectrum (400 – 750 nm), chitosan (100:0 CH:AL) film exhibited the best light transmission and alginate (0:100 CH:AL) film displayed a very close degree of light transmission to chitosan. This occurred due to the intrinsic yellowish hue of alginate. However, the films prepared by means of different composition (80:20, 60:40, 50:50, 40:60 CH:AL) exhibited lower light transmission property than pure films. Possible ionic complexation between chitosan and alginate induced an impact on the transparency of the composite films, thus lessened their light transmission ratio. In addition, 80:20 CH:AL film exhibited the worst property due to the precipitation of the alginate. Nevertheless, except 80:20 CH:AL film, the light transmission ratio of all films is still above 86%, indicating high transparency.

It can be also clearly observed from Figure 2.8 that the 50:50 CH:AL film is highly transparent, which is already confirmed by light transmission measurements.

Figure 2. 8 50:50 CH:AL film

2.3.4 Infrared spectroscopy

FTIR spectra of 60:40 CH:AL film and pure samples are observed in Figure 2.9. The characteristic absorption bands at 1637 and 1542 cm^{-1} represent the amide I and amide II band respectively on chitosan films (Table 2.3) (Lawrie et al., 2007). For alginate, the absorption bands at 1592 cm^{-1} and 1407 cm^{-1} represent the anti-symmetric and symmetric stretching vibrations of $-COO^-$ (Table 2.3). Lawrie et al. (2007) also reported similar results on the absorption bands of chitosan and alginate.

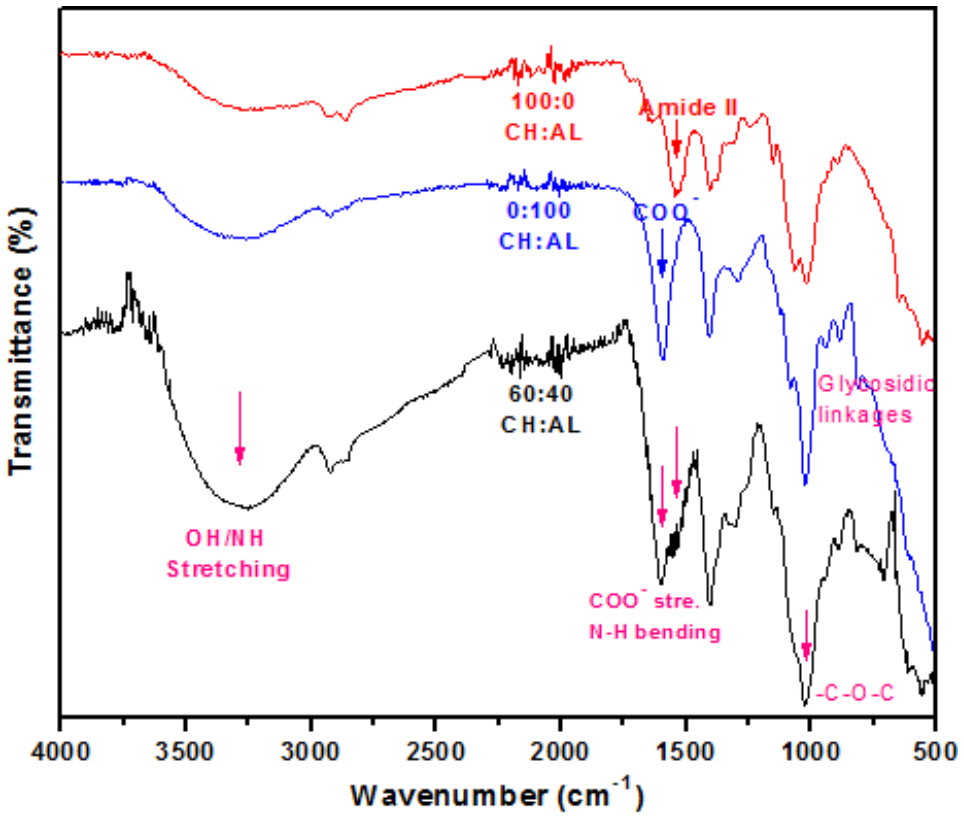

Figure 2. 9 FTIR spectra of chitosan (100:0), alginate (0:100) and 60:40 CH:AL films

Table 2. 3 FTIR bands of chitosan, alginate and 60:40 CH:AL films with assignments

100:0 CH:AL Vibration (cm^{-1})	**Assignment**
3350-3000	O-H and N-H stretch
2875	C-H stretch
1637	Amide I
1542	N-H bending from amine and amide II
1405	$-CH_2$ bending
1376	CH_3 symmetrical deformation
1151	Antisymmetric C-O-C stretch and C-N stretch
1064-1018	Skeletal vibration of C-O stretching

0:100 CH:AL Vibration (cm^{-1})	**Assignment**
3600-3000 (broad)	O-H stretch
2930	C-H stretch
1592	Antisymmetric COO^- stretch
1407	Symmetric COO^- stretch
1295	Skeletal vibration
1081-1024	Antisymmetric C-O-C stretch
60:40 CH:AL Vibration (cm^{-1})	**Assignment**
3500-3000 (broad)	O-H and N-H stretch
2923	C-H stretch
1597	Antisym COO^- stretch
1540	N-H bending from amide II
1400	Sym COO^- stretch or -CH2 bending
1305	skeletal vibration
1149	Antisym C-O-C stretch and C-N stretch
1064-1024	Skeletal vibration of C-O stretching

The absorption bands of 60:40 CH-AL film reveal similar characteristics with both chitosan (100:0 CH:AL) and alginate (0:100 CH:AL) films. The O-H and $-NH_2$ groups in chitosan may form hydrogen bonds with -C=O and -OH groups of alginate. The absorption band at 1542 cm^{-1} in chitosan shifted to 1540 cm^{-1} and 1592 cm^{-1} in alginate shifted to 1590 cm^{-1} after alginate reacted with $-NH_2$ groups via hydrogen bonds (Table 2.3). Due to the same probable bonding, two similar peaks, one in chitosan at 1405 cm^{-1}

and the other in alginate at 1407 cm^{-1} overlap each other in the 60:40 CH:AL sample (Table 2.3). The composite film also shows characteristic absorption bands between 3000 cm^{-1} and 3600 cm^{-1}, which represent the -OH and -NH_2 groups in free as well as in amide form in chitosan (Meng et al., 2009). Additionally, ionic interactions most likely occurred between chitosan and alginate. The cationic $-\mathrm{NH}_3^+$ group in chitosan and anionic $-\mathrm{COO}^-$ group in alginate are capable of forming complexes with opposite charges. Therefore, these intermolecular interactions result in forming polyelectrolyte complex (Meng et al., 2009).

2.3.5 Thermal analysis

Figure 2.10 and 2.11 show the TGA and DSC thermograms of 50:50, 100:0, 0:100 CH:AL films. For all samples, weight loss took place in two stages. The first one starts at ~50°C with a weight loss of 10% and reaches a maximum above 100°C. This stage is assigned to water evaporation.

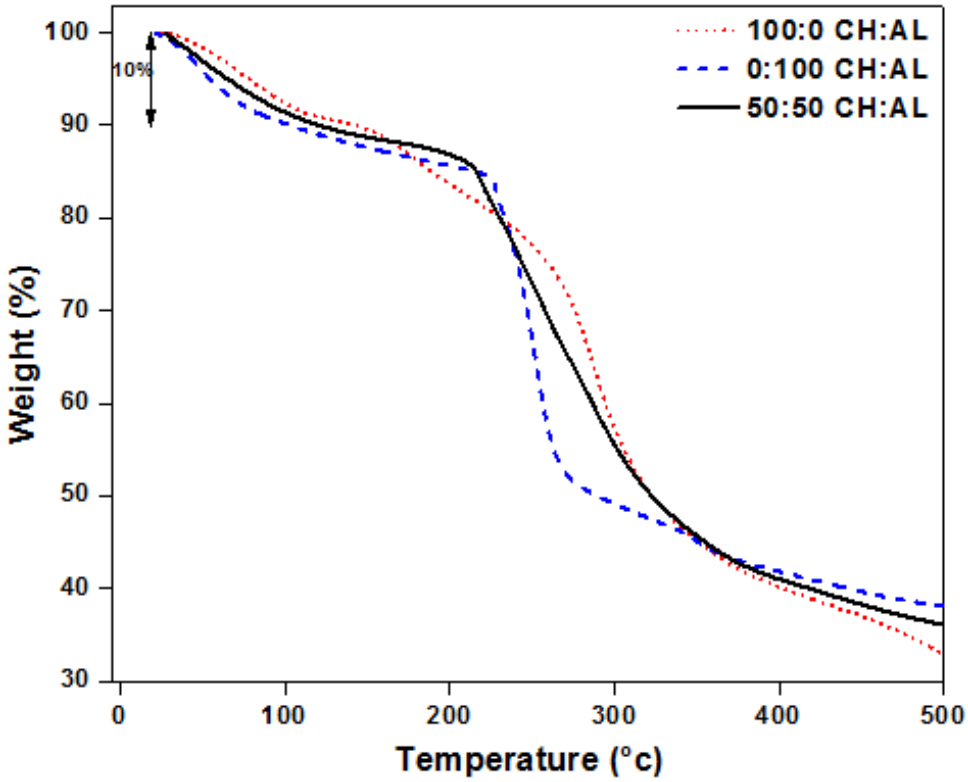

Figure 2. 10 TGA thermograms of chitosan (100:0 CH:AL), alginate (0:100 CH:AL) and 50:50 CH:AL films

The second stage for chitosan occurs at 300°C with a weight loss of above 40%. This result is similar to the findings of Nieto et al. (1991) and Tirkistani (1998). For alginate, this stage takes place at 250°C with a weight loss of ~35%. Çaykara et al. (2005) and Parhi et al. (2006) reported similar results for alginate. This stage corresponds to the decomposition (thermal and oxidative) of chitosan and alginate, vaporization and elimination of volatile products. According to Nieto et al. (1991), pyrolysis of polysaccharides starts by a random split of the glycosidic bonds, followed by a further decomposition forming acetic and butyric acids and a series of lower fatty acids, where C2, C3 and C6 predominate.

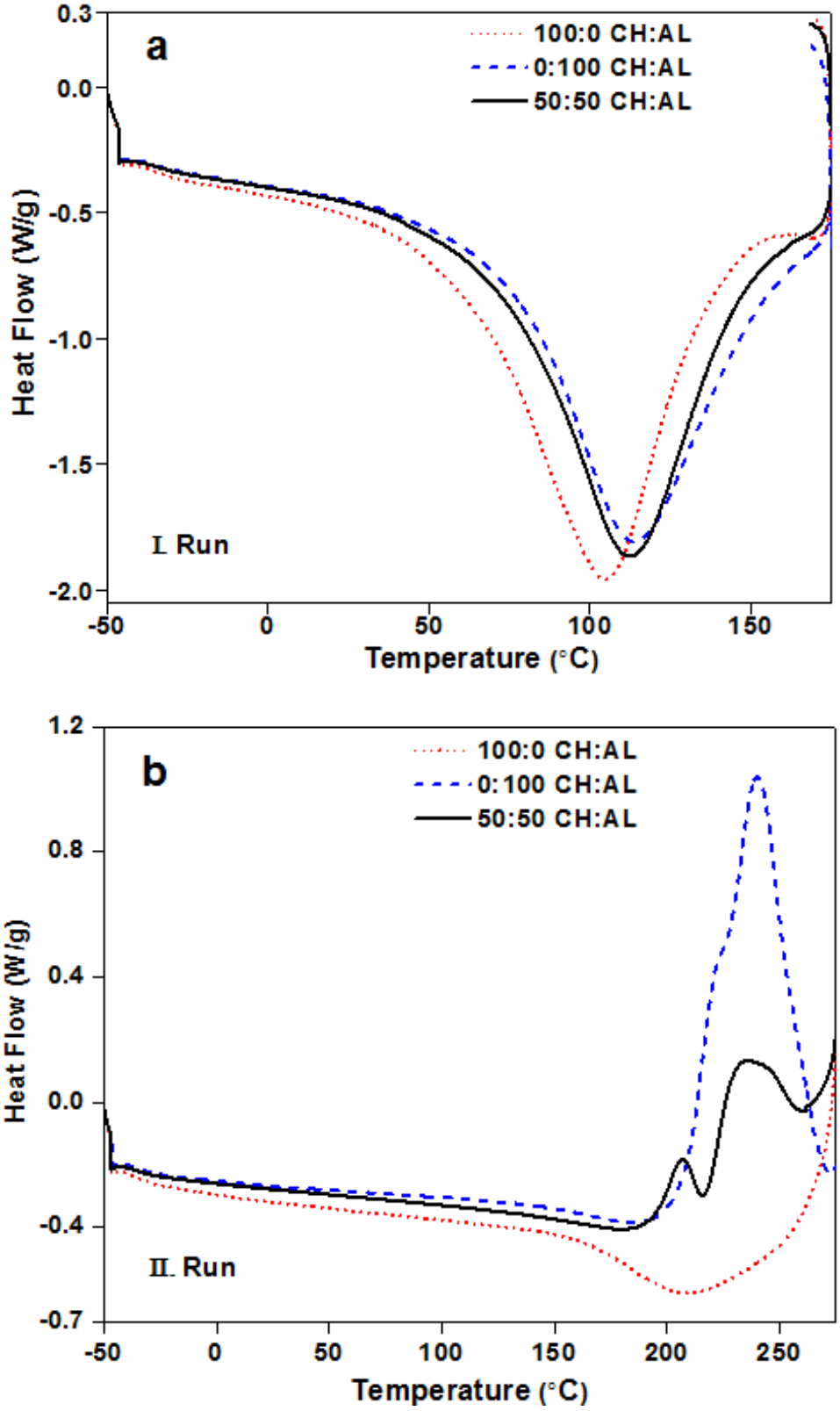

Figure 2. 11 DSC thermograms of chitosan (100:0 CH:AL), alginate (0:100 CH:AL), and 50:50 CH:AL films. a) first run b) second run

The composite (50:50 CH:AL) film shows the characteristic of both chitosan and alginate films. The second stage for this film starts at 204°C and reaches a maximum at 380°C. It undergoes a broad range of decomposition due to its components. Therefore, this binary polysaccharide includes the thermal history of chitosan and alginate and its decomposition stage can be attributed to the same explanation expressed by Nieto et al. (1991).

The first heating (Figure 2.11(a)) process on DSC thermogram shows a large endothermic peak above 100°C indicating solvent evaporation (mainly water) of all films. This is also in agreement with the TGA results. The second heating (Figure 2.11(b)) process was applied after all solvent traces were eliminated. Its thermogram shows degradation of all films above 200°C. For example, the 50:50 mixture film starts degrading around 204°C which is also the same temperature found in TGA results.

Because no glass transition is observed on calorimetric data dynamic mechanical analysis (DMA) was performed for films. DMA tests were performed using two heating processes. The first heating was applied in order to eliminate the effect of residual water. After holding the samples at 110°C for ten minutes, no color change observed. However, all samples shrunk almost 10% in every dimension. The shrinkage can be attributed to the [10%] weight loss observed on TGA. After the first heating, second heating was applied with 0.01% strain. Figure 2.12 displays the dynamic mechanical spectra on storage modulus, *E*', and tan δ of samples, acquired from the DMA measurement during the second heating process.

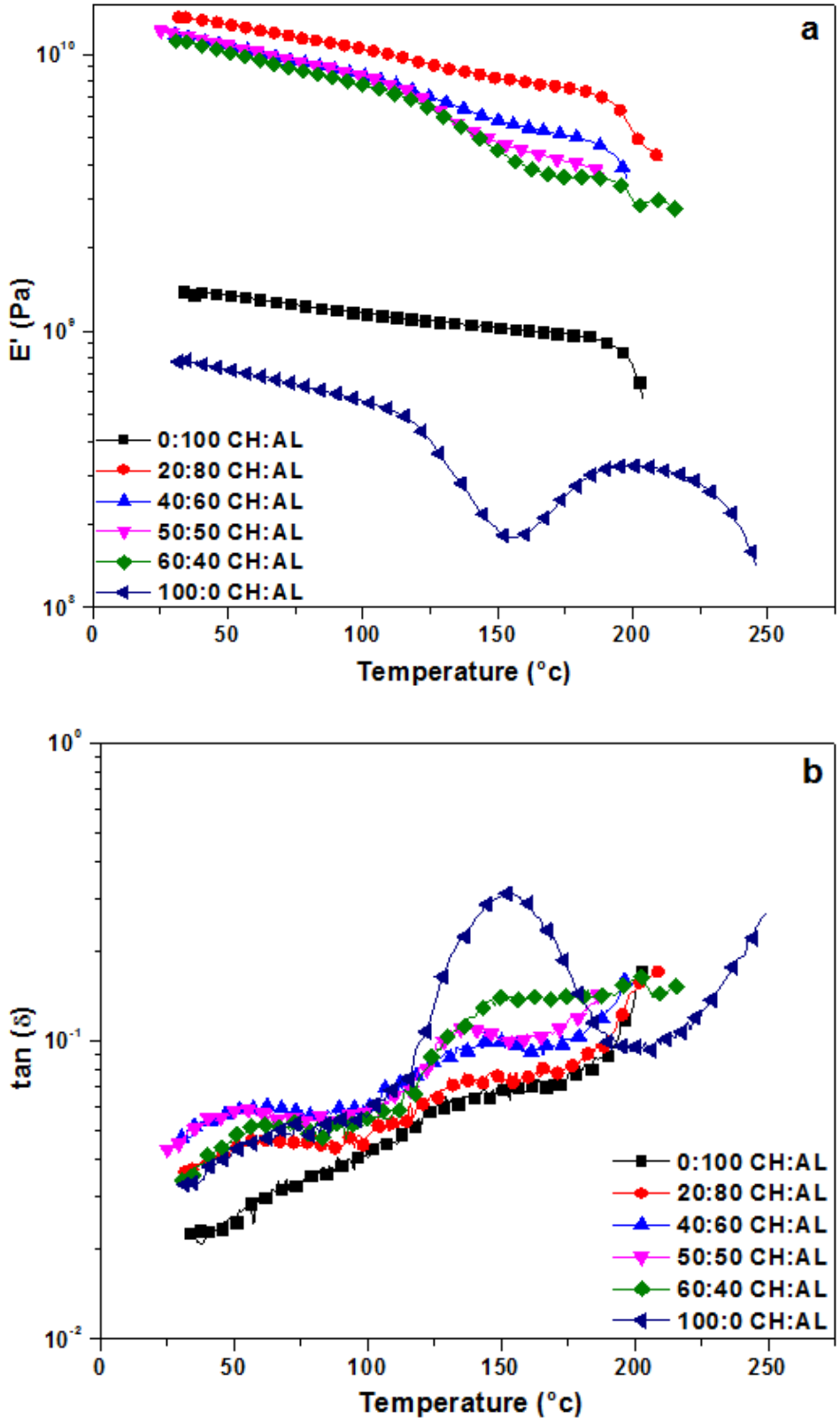

Figure 2. 12 Dynamic temperature ramp test of films: a) E' (storage modulus), b) tan δ versus temperature

A sharp peak at 155°C is observed on tan δ or curve deflection on *E'* for pure chitosan (100:0 CH:AL) sample during the second heating which corresponds to the relaxation process of the chitosan network. Similar results were reported by Mucha and Pawlak (2005). Furthermore, no related transition occurred on pure alginate. Although chitosan and alginate have similar structures based on glycosidic bonds, alginate did not exhibit any transition other than molecular degradation after 195°C. Mitchell (1998) explains this with chain mobility which in biopolymers occurs less often than most synthetic polymers. Two reasons stand out for this in polysaccharides. First, steric hindrances intensively affect the open angles of rotation on the glycosidic bond, the geometry of which mostly provides that restriction. Second, some intra chain attractive interactions, particularly hydrogen bonding, will also limit the mobility. Because glass transition depends on chain mobility, a clear transition less likely occurs in immobilized polymers through other mechanisms (Mitchell, 1998).

It can be clearly noticed that there is a tendency on both graphs at 155°C through the rise of chitosan content in each composite film. The peak becomes much clearer as the percentage of the chitosan in composite films increases. Therefore, composite films exhibit a transition due to the chitosan segment.

It is remarkable that the storage moduli (*E'*) of all composite films increased around one order of magnitude compared to pure films. This most likely occurred though stronger interaction between chitosan and alginate after the solvent evaporation. When water induced hydrogen bonding replaced with more ionic interaction between the two polymers, the binary polysaccharide network became more compact and more binding were obtained.

2.3.6 Morphology of the films

The surface morphology of the chitosan alginate composite films was observed with scanning electron microscopy to verify the compatibility of the mixtures of alginate and chitosan. Figure 2.13 shows the fractured surface of the pure and composite films.

The cross section structure of alginate film (0:100 CH:AL) is very rough compared to that of chitosan film (Figure 2.13(a, b) and 2.13(e, f)). This difference can also be observed in the composite film (Figure 2.13(c, d)) which two biopolymers formed mainly a two-phase system. Although the presence of phase separation at a microscopic level was detected for the composite films, pronounced interactions between two components can be confirmed by their solubility. After the composite films are dried, they cannot be dissolved completely in water again because of the polyionic complexation.

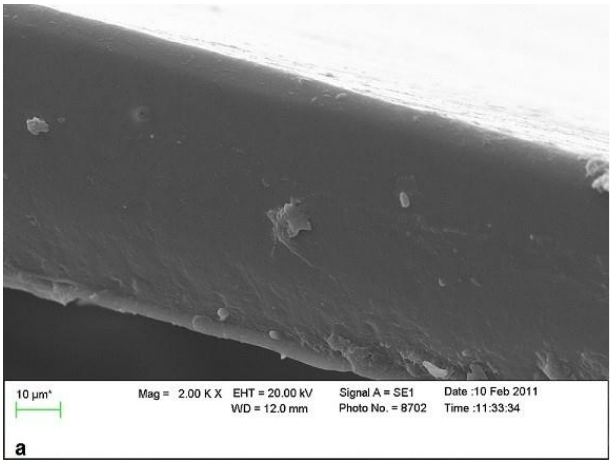

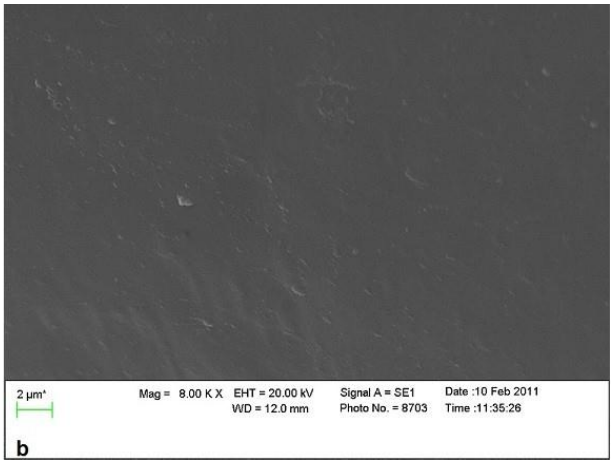

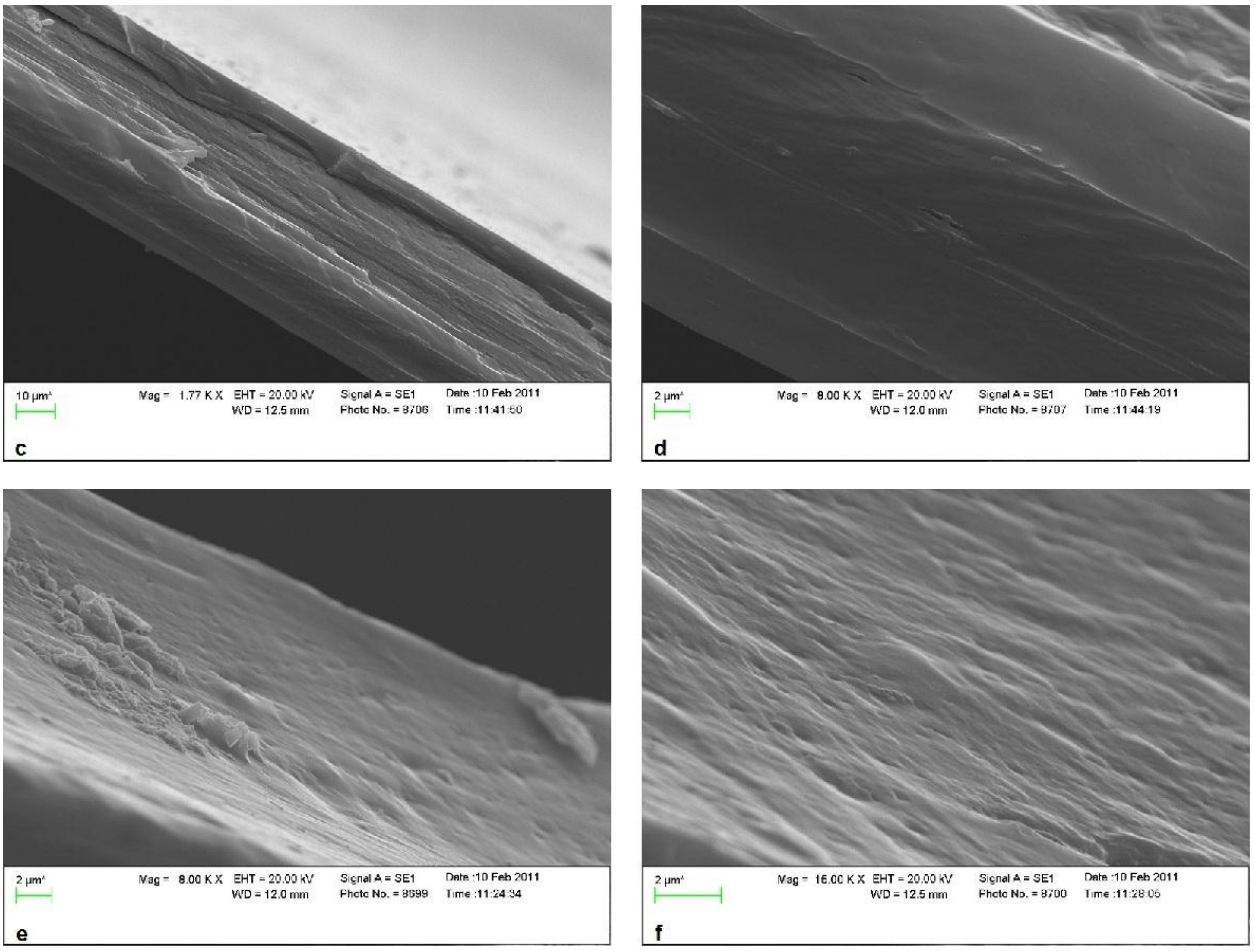

Figure 2. 13 SEM pictures of a, b) 100:0 CH:AL, c, d) 50:50 CH:AL and e, f) 0:100 CH:AL films

It is well-known that a better mixture could be achieved if the concentration of the each solution is reduced accordingly. However, in our study, it was observed that lower than 1.0 w/v% concentrations of either of the component solutions creates precipitation in one another. Consequently, the resulting films cast from the mixed solutions will possess a macroscopically phase separated structure and exhibit an immiscible appearance.

Even though phase separation and layered structure were observed on our composite films, the transparency was not affected. This is a result of the refractive

index of both phases which are polysaccharides. They ($n_{Chitosan}$= 1.59, $n_{Alginate}$= 1.507) have similar refractive indexes (Ligler et al., 2001, Cathell and Schauer, 2007).

2.3.7 Mechanical properties

In this study, aqueous acetic solution was used as a casting solution. Relatively warm air (30°C) evaporates water from the outermost region of the initial mixture to induce film to dry and finally form a dense uniform skin. As is also shown in Figure 2.8, the 50:50 CH:AL film exhibits a miscible appearance. However, the microscopic evidence revealed phase separation of the two polymer networks, with phase inversion occurring at each composition. As a result, all films prepared are symmetric and layer-by-layer phase separated except the 80:20 CH:AL film in which alginate precipitates due to lack of interaction with chitosan.

The Young's modulus, deformation at break, yield strength and stress at break of the chitosan-alginate composite films with various chitosan content were tested according to the ASTM D638-94b (1994) and the results are reported in Figure 2.14 and Table 2.4.

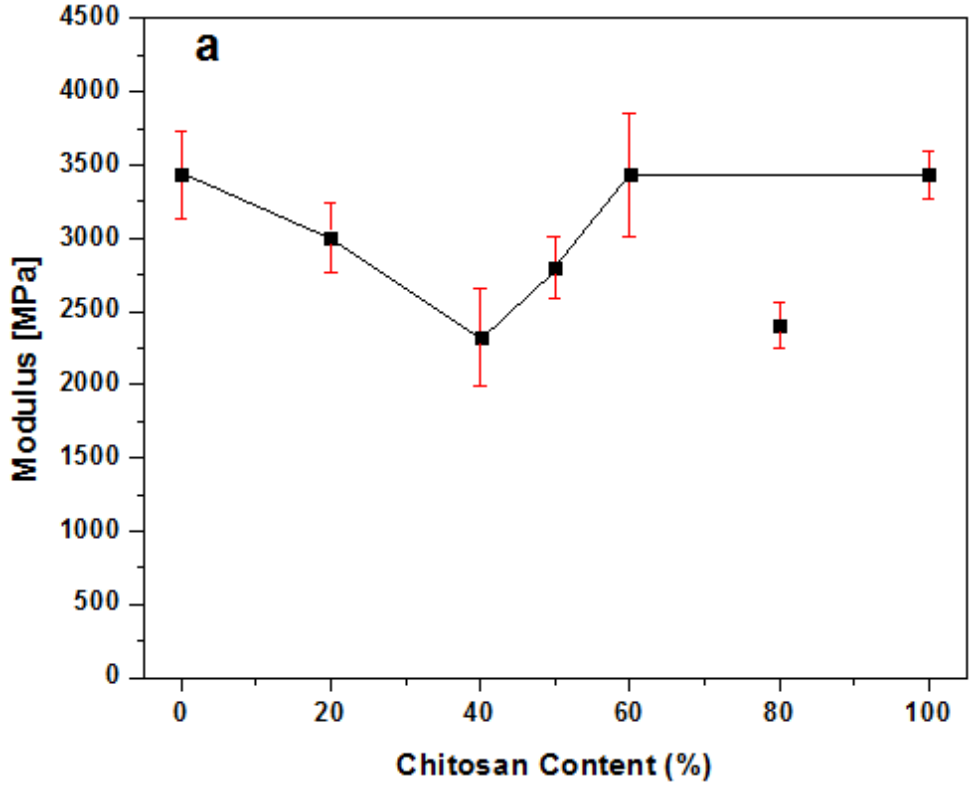
a
Modulus [MPa]
4500
4000
3500
3000
2500
2000
1500
1000
500
0
0
20
40
60
80
100
Chitosan Content (%)

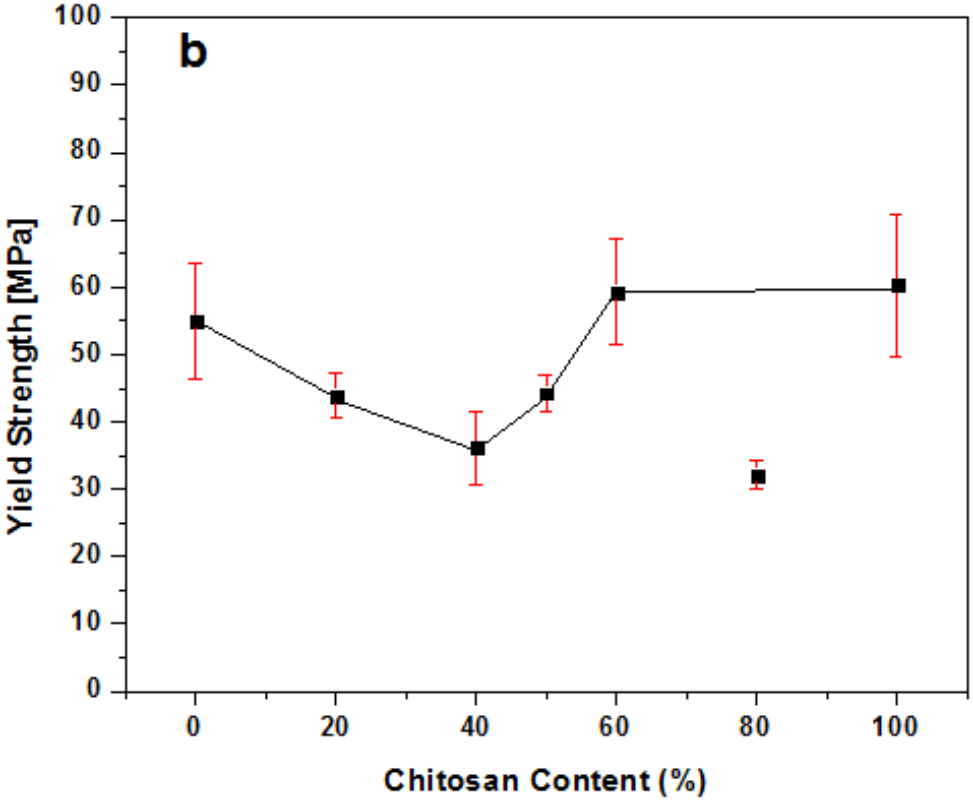
b
Yield Strength [MPa]
100
90
80
70
60
50
40
30
20
10
0
0
20
40
60
80
100
Chitosan Content (%)

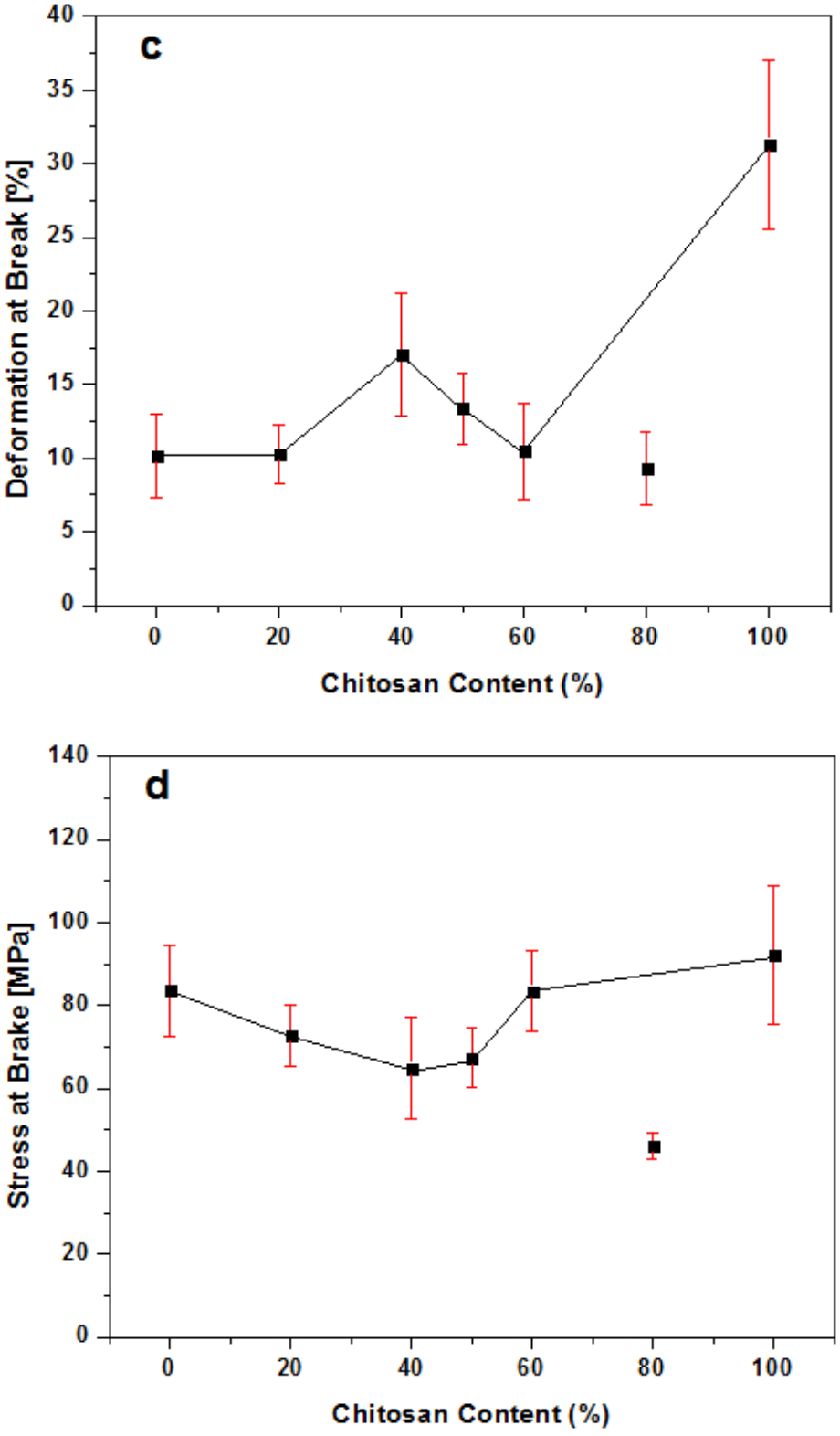

Figure 2. 14 Mechanical properties of chitosan-alginate films: a) Modulus, b) Yield strength, c) Deformation at break, d) Stress at break

All the composite films showed similar mechanical behaviors but the one with chitosan content of 80% due to the precipitation of alginate. The mechanical results of this film on all graphs excluded as an exception to the composite films produced.

The stress at break, yield strength and Young's modulus of composite films reach a maximum at 60% chitosan content indicating the greatest ionic interaction among all composite films. Because tensile tests were conducted without evaporating water content of the films, we could not observe any increase on the modulus of composite films as we did in their storage moduli. Although phase separation was observed, composite films possess hydrogen bonding and ionic interaction through the interface of each component. As a result, the toughest composition was obtained in 60:40 CH:AL film which has nearly the same modulus as chitosan (100:0 CH:AL) and alginate (0:100 CH:AL) films.

Table 2. 4 Mechanical properties of chitosan-alginate films

Films CH-AL	Young's Modulus (MPa)	Deformation at Break (%)	Yield Strength (MPa)	Stress at Break (MPa)
0:100	3433 ± 302	10.17 ± 2.85	54.93 ± 8.57	83.53 ± 11.07
20:80	3007 ± 236	10.26 ± 2.04	43.89 ± 3.41	72.64 ± 7.41
40:60	2323 ± 330	17.0 ± 4.18	36.14 ± 5.37	64.84 ± 12.28
50:50	2800 ± 210	13.35 ± 2.48	44.23 ± 2.75	67.30 ± 7.25
60:40	3432 ± 423	10.47 ± 3.24	59.29 ± 7.76	83.44 ± 9.89
80:20	2404 ± 150	9.28 ± 2.49	32.10 ± 2.08	46.05 ± 3.09
100:0	3430 ± 168	31.25 ± 5.74	60.27 ± 10.57	92.06 ± 16.70

Chitosan and alginate films show good breaking strength, but alginate film show lower deformation at break as shown in Figure 2.14. The tendency with the increase of chitosan content between Young's modulus and deformation at break is slightly contrary. 60:40 CH:AL film has low deformation at break along with 20:80 CH:AL and 0:100 CH:AL films. There is also the same tendency for all films in Young's modulus, yield strength and stress at break.

Arvanitoyannis et al. (1998) produced films from a binary polysaccharide network composed of 2 w/v% chitosan and 5 w/v% gelatin. They cast phase separated and 08±0.06 mm thick films which are much thicker than our films. In addition, the 50:50 composite film has 2050±200 MPa modulus and 4.1±0.5 % deformation at break. In comparison with the same ratio of our composite film, we obtained higher values in terms of modulus and deformation at break.

2.3.8 Antibacterial testing - Zone of inhibition test

The antibacterial behaviors of films with composition of 100:0, 60:40, 80:20 and 0:100 CH:AL were evaluated and the results were reported whether there is inhibition zone of bacterial growth at the film/medium interface. Figure 2.15 shows that the chitosan (100:0 CH:AL) film itself and the 80% and the higher content of chitosan containing composite films could inhibit the bacterial growth at the interface.

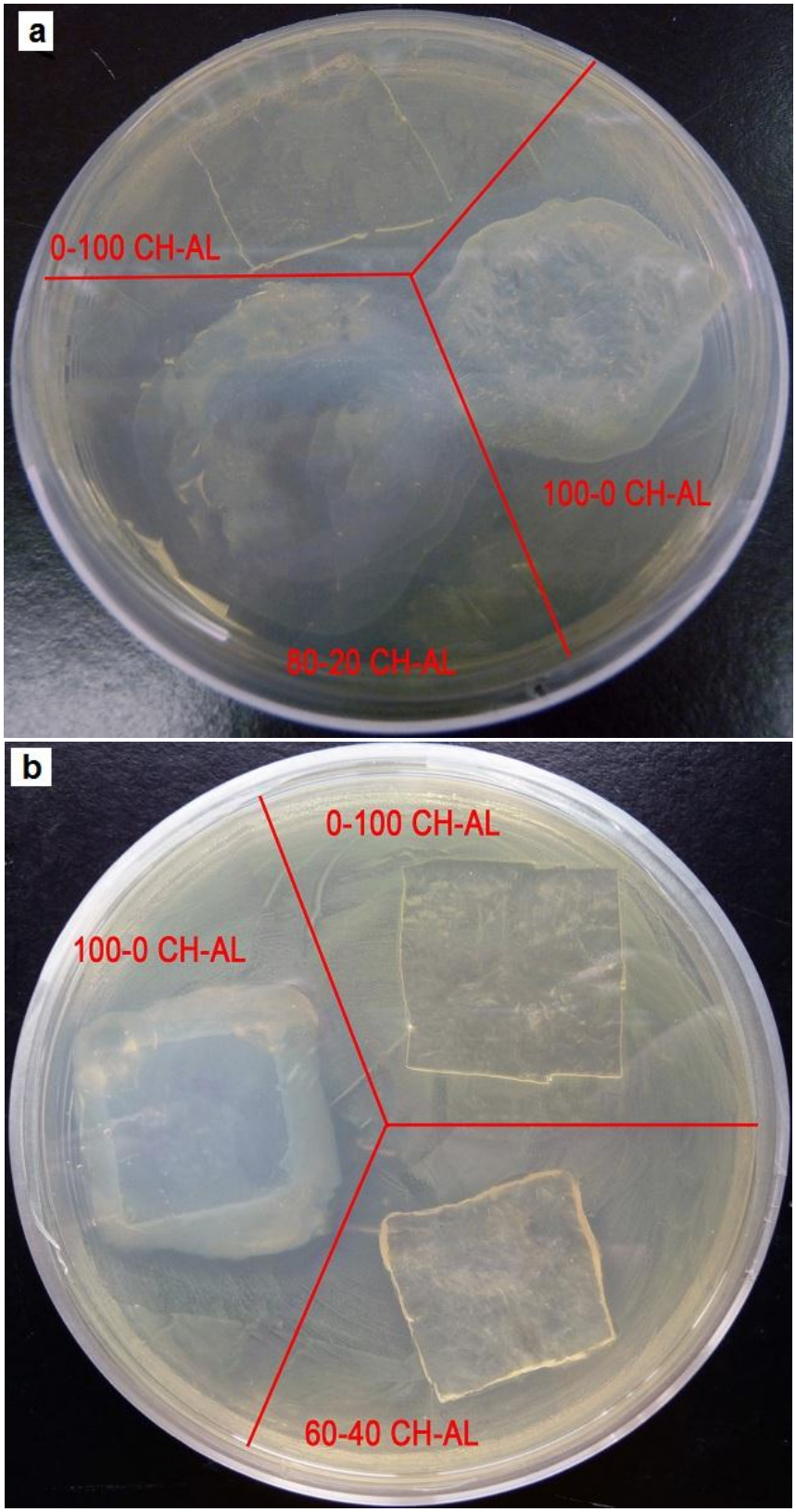

Figure 2. 15 Representative picture of inhibitory effect of the selected films: 100:0, 60:40, 80:20 and 0:100 CH:AL films

Alginate film is taken as a reference sample on account of its non-bioactivity against bacteria. Based on the charge potential of the films, the composite films have a decreased number of charges as a result of the possible ionic interaction of polycationic chitosan and polyanionic alginate. Consequently, the film with a lower content of chitosan such as 60% does not exhibit any biocidal activity. Tsai et al. (2002) investigated that the antibacterial action of chitosan increases with the increase of deacetylation degree (DD) of chitosan. So 80% DD of chitosan is the most apparent reason that the expected antibacterial activity vanishes in composite films with higher than 50% of chitosan. This effect of DD in chitosan-alginate composition is overcome through a greater content of chitosan such as 80% and 90%.

The antibacterial mechanism of chitosan is still unknown. However, different approaches have been suggested. Rabea et al. (2003) reported that interaction between $–NH_3^+$ of chitosan and negatively charged bacterial cell membranes causes the leakage of proteinaceous and other intracellular constituents. Chitosan was mostly effective on the outermost surface of the bacteria (Rabea et al., 2003). At a low concentration (<0.2 mg/mL), the positively charged chitosan likely binds to the anionic bacterial surface to induce agglutination, whereas at high concentrations, more positive charges might give a final positive charge to the bacterial surfaces to maintain them in suspension (Rabea et al., 2003).

2.4 CONCLUSION

Our NMR results confirmed that the deacetylation degree of chitosan used is ~80%. Through zeta potential measurement, we observed that in a mixture solution of chitosan and alginate, the net charge of the system decreased due to polyelectrolyte complexation. After preparing the composite films, their transparency did not show significant change due to the complexation compared to either chitosan or alginate film. FTIR spectroscopy of the composite films showed that characteristic absorption bands of each one of the polymers shifted which indicated an ionic interaction between chitosan and alginate.

Thermogravimetric analyses of the selected films revealed degradation and decomposition of the biopolymers following the evaporation of water. Calorimetric analyses were in agreement with TGA analyses but showed no indication of glass transition and melting temperature of any of the biopolymers used. On DMA results, a transition peak at 155°C of chitosan film was also observed and intensified with increase of chitosan content in the composite films. However, none of the results was a proof of glass transition and melting temperature. Additionally, the storage moduli of composite films increased due to strong polyelectrolyte complexation between the two polysaccharides without 10% water content.

Even though the composite films have a miscible appearance, SEM pictures displayed that they are phase separated at a microscopic level. Mechanical behaviors of the films revealed that 60:40 CH:AL film was the ideal composition for chitosan and alginate components. Finally, antibacterial activity of the composite films was found in

80:20 CH:AL film in which positive charged amine groups are more available to kill the bacteria.

REFERENCES

ARVANITOYANNIS, I., KOLOKURIS, I., NAKAYAMA, A., YAMAMOTO, N. & AIBA, S. 1997. Physico-chemical studies of chitosan-poly (vinyl alcohol) blends plasticized with sorbitol and sucrose. *Carbohydrate Polymers,* 34**,** 9-19.

ARVANITOYANNIS, I. S., NAKAYAMA, A. & AIBA, S. 1998. Chitosan and gelatin based edible films: state diagrams, mechanical and permeation properties. *Carbohydrate Polymers,* 37**,** 371-382.

ASTM 1993. Standard test method for tensile properties of Plastics by use of microtensile specimens, Standards Designation: D882. In Annual Book of ASTM Standards. Philadelphia, USA: ASTM. p 374.

ASTM 1994. Standard test method for tensile properties of Plastics, Standards Designation: D638. In Annual Book of ASTM Standards. Philadelphia, USA: ASTM. p 47.

CATHELL, M. D. & SCHAUER, C. L. 2007. Structurally colored thin films of Ca2+-cross-linked alginate. *Biomacromolecules,* 8**,** 33-41.

ÇAYKARA, T., DEMIRCI, S., EROGLU, M. S. & GÜVEN, O. 2005. Poly (ethylene oxide) and its blends with sodium alginate. *Polymer,* 46**,** 10750-10757.

CERVERA, M. F., KARJALAINEN, M., AIRAKSINEN, S., RANTANEN, J., KROGARS, K., HEINAMAKI, J., COLARTE, A. I. & YLIRUUSI, J. 2004. Physical stability and moisture sorption of aqueous chitosan-amylose starch films plasticized with polyols. *European journal of pharmaceutics and biopharmaceutics,* 58**,** 69-76.

CHATTERJEE, S. K., GUPTA, S. & SETHI, K. R. 1987. Study of CU(II)-methacrylic acid — methacrylamide copolymer interactions and formation of metal-copolymer complexes. *Die Angewandte Makromolekulare Chemie,* 147**,** 133-146.

DRAGET, K., PHILLIPS, G. & WILLIAMS, P. 2009. Alginates. *Handbook of hydrocolloids***,** 807-828.

GEORGE, M. & ABRAHAM, T. E. 2006. Polyionic hydrocolloids for the intestinal delivery of protein drugs: alginate and chitosan--a review. *Journal of Controlled Release,* 114**,** 1-14.

HIRAI, A., ODANI, H. & NAKAJIMA, A. 1991. Determination of degree of deacetylation of chitosan by 1 H NMR spectroscopy. *Polymer Bulletin,* 26**,** 87-94.

KOLODZIEJSKA, I. & PIOTROWSKA, B. 2007. The water vapour permeability, mechanical properties and solubility of fish gelatin-chitosan films modified with transglutaminase or 1-ethyl-3-(3-dimethylaminopropyl) carbodiimide (EDC) and plasticized with glycerol. *Food chemistry,* 103**,** 295-300.

LAWRIE, G., KEEN, I., DREW, B., CHANDLER-TEMPLE, A., RINTOUL, L., FREDERICKS, P. & GRØNDAHL, L. 2007. Interactions between alginate and chitosan biopolymers characterized using FTIR and XPS. *Biomacromolecules,* 8**,** 2533-2541.

LAZARIDOU, A. & BILIADERIS, C. G. 2002. Thermophysical properties of chitosan, chitosan-starch and chitosan-pullulan films near the glass transition. *Carbohydrate Polymers,* 48**,** 179-190.

LIGLER, F. S., LINGERFELT, B. M., PRICE, R. P. & SCHOEN, P. E. 2001. Development of uniform chitosan thin-film layers on silicon chips. *Langmuir,* 17**,** 5082-5084.

MENG, X., TIAN, F., LI, F., XING, N. & YANG, J. 2009. Study on the Blending Solution Behavior and Membrane Properties of Sodium Alginate and Chitosan. IEEE.

MITCHELL, J. 1998. *Water and food macromolecules*, Aspen Publishers: Gaithersburg, MD.

MIYA, M., IWAMOTO, R., YOSHIKAWA, S. & MIMA, S. 1980. I.r. spectroscopic determination of CONH content in highly deacylated chitosan. *International journal of biological macromolecules,* 2**,** 323-324.

MUCHA, M. & PAWLAK, A. 2005. Thermal analysis of chitosan and its blends. *Thermochimica acta,* 427**,** 69-76.

NETO, C., GIACOMETTI, J., JOB, A., FERREIRA, F., FONSECA, J. & PEREIRA, M. 2005. Thermal analysis of chitosan based networks. *Carbohydrate Polymers,* 62**,** 97-103.

NIETO, J., PENICHE-COVAS, C. & PADRO'N, G. 1991. Characterization of chitosan by pyrolysis-mass spectrometry, thermal analysis and differential scanning calorimetry. *Thermochimica acta,* 176**,** 63-68.

PARHI, P., RAMANAN, A. & RAY, A. R. 2006. Preparation and characterization of alginate and hydroxyapatite based biocomposite. *Journal of Applied Polymer Science,* 102**,** 5162-5165.

PEREDA, M., ARANGUREN, M. I. & MARCOVICH, N. E. 2008. Characterization of chitosan/caseinate films. *Journal of Applied Polymer Science,* 107**,** 1080-1090.

RABEA, E. I., MOHAMED, E. T. B., STEVENS, C. V., SMAGGHE, G. & STEURBAUT, W. 2003. Chitosan as antimicrobial agent: applications and mode of action. *Biomacromolecules,* 4**,** 1457-1465.

RHIM, J. W. & NG, P. K. W. 2007. Natural biopolymer-based nanocomposite films for packaging applications. *Critical reviews in food science and nutrition,* 47**,** 411-433.

SANNAN, T., KURITA, K., OGURA, K. & IWAKURA, Y. 1978. Studies on chitin: 7. I.r. spectroscopic determination of degree of deacetylation. *Polymer,* 19**,** 458-459.

SRINIVASA, P. & THARANATHAN, R. 2007. Chitin/Chitosan—Safe, Ecofriendly Packaging Materials with Multiple Potential Uses. *Food Reviews International,* 23**,** 53-72.

TAKAHASHI, T., TAKAYAMA, K., MACHIDA, Y. & NAGAI, T. 1990. Characteristics of polyion complexes of chitosan with sodium alginate and sodium polyacrylate. *International Journal of Pharmaceutics,* 61**,** 35-41.

TERAYAMA, H. 1952. Method of colloid titration (a new titration between polymer ions). *Journal of Polymer Science,* 8**,** 243-253.

TIRKISTANI, F. A. A. 1998. Thermal analysis of some chitosan Schiff bases. *Polymer degradation and stability,* 60**,** 67-70.

TSAI, G., SU, W., CHEN, H. & PAN, C. 2002. Antimicrobial activity of shrimp chitin and chitosan from different treatments and applications of fish preservation. *Fisheries Science,* 68.

VÅRUM, K. M., ANTOHONSEN, M. W., GRASDALEN, H. & SMIDSRØD, O. 1991. Determination of the degree of N-acetylation and the distribution of N-acetyl groups in partially N-deacetylated chitins (chitosans) by high-field nmr spectroscopy* 1. *Carbohydrate research,* 211**,** 17-23.

XU, Y., KIM, K. M., HANNA, M. A. & NAG, D. 2005. Chitosan-starch composite film: preparation and characterization* 1. *Industrial Crops and Products,* 21**,** 185-192.

ZACTITI, E. & KIECKBUSCH, T. 2006. Potassium sorbate permeability in biodegradable alginate films: Effect of the antimicrobial agent concentration and crosslinking degree. *Journal of food engineering,* 77**,** 462-467.

ZHAI, M., ZHAO, L., YOSHII, F. & KUME, T. 2004. Study on antibacterial starch/chitosan blend film formed under the action of irradiation. *Carbohydrate Polymers,* 57**,** 83-88.

CHAPTER THREE

CHITOSAN AND ALGINATE WET SPUN FIBERS

3.1 INRODUCTION

Fibers produced from renewable resources, in particular polysaccharides, have drawn considerable attention for their outstanding biocompatibility, non-toxicity, biodegradability and intrinsic bioactivity in applications, such as wound management, tissue engineering, and drug delivery (Knill et al., 2004, Tuzlakoglu and Reis, 2008, Liao et al., 2005). The number of studies on alginate and chitosan as polysaccharide biopolymers has been expanding due to their potential use in biomedical applications.

Fibers have been widely utilized in biomedical applications on account of their typical favorable properties, for instance, large surface area, softness, high porosity, and ease of production into many forms (Knill et al., 2004). Several commercial wound dressing materials (woven and non-woven dressings and hydrogels) have been manufactured from polysaccharides and their derivatives. For example, support and compression bandages, absorbents, gauzes, tulle dressings, and wound dressing pads are made from woven cellulose fibers (cotton and viscose) (Kennedy et al., 1996, Lloyd et al., 1998, Kennedy and Thoriey, 2001, Knill et al., 2004).

The favorable properties (mentioned earlier) of biodegradable fiber structures can be modified for specific applications (Tuzlakoglu and Reis, 2008). For instance, they can replace many tissues, such as nerve, muscle, tendon, ligament, blood vessel, bone,

and teeth which already have cannular or fiber-shaped architectures and anti-symmetric properties. Therefore, fiber-based structures can generate a myriad of applications in tissue engineering. On the other hand, numerous factors must be taken into account in the fiber design for such applications, such as ideal fiber diameter and linear mass, overall absorbency and the distribution of pore size, effect of fiber orientation on response of cells, and effect of degradation on the properties of the structures (Tuzlakoglu and Reis, 2008).

Liao et al. (2005) suggested that polyelectrolyte complex fibers comprised of chitosan and alginate can be used to control drug or and protein release. Compared to microparticule and bead systems, there are less parameters, such as complexation and the drawing ratio of fibers affecting protein entrapment efficacy and release behaviors. Besides that, drug loading process does not require complicated process stages. However, the molecule of target must possess ionic charge groups in order to obtain continuous drug delivery. Overall, the polyelectrolyte complex fibers could be a promising drug deliverer with the benefits of high effective encapsulation, high loading level, sustained release profile, and continuum of the activity of biomolecules (Liao et al., 2005).

Chitosan based materials (details given in Chapter 1) can be generated as powder, films, beads, fibers, and fabrics (Qin and Agboh, 1998). However, materials produced from pure chitosan fibers have not been practically applicable as a result of their insufficient tensile properties and the relatively high production costs (Watthanaphanit et al., 2009). Furthermore, pure chitosan is currently not accessible for a mass production of those fibers (Watthanaphanit et al., 2009). Another disadvantage

of chitosan is its poor solubility in water which limits its applicability as a polysaccharide drug. Although this drawback can be overcome through chemical modifications (Kurita et al., 1998), the complexity of reaction process and the relatively high cost of manufacturing final product are usually the main disadvantages (Watthanaphanit et al., 2009).

Alginate fibers have also been produced and specifically used in wound management (Qin, 2008). Because of alginate's high water absorbency and insolubility generated by the present of divalent cations, such as Ca^{2+}, alginate-based fiber mats was produced as a wound dressing application (Aogren, 1996). However, as previously stated, alginate does not possess an intrinsic antibacterial property thereby wounds may not be sterilized form colonization of microorganisms, which may cause infection and hinder healing, through that of fiber mat. Nevertheless, integration of chitosan into alginate or vice versa could improve the properties of the fibers with the either one of the component. The interaction between these two biopolymers enables the development of tailored bio-fibers through their potential to form a polyelectrolyte complex via ionic interactions.

There are some examples of mixture of individually assembled alginate and chitosan fibers. Pandit (1998) produced alginate and chitosan staple fibers separately and then blended in order to achieve a nonwoven wound dressing. Cole and Nelson (1993) employed chitosan as the cationic core for the production of an alginate fiber. Tamura et al. (2002) coated of chitosan on alginate filament and Knill et al. (2004) and Niekraszewicz et al. (2006) independently obtained a fiber of which alginate is the core and chitosan is the skin. Knill et al. (2004) proved that adsorption of chitosan into

alginate fiber or coating onto an alginate filament core could be elevated via hydrolization. Due to the better mobility of the hydrolyzed chitosan chains, the amount of chitosan incorporation increases (Knill et al., 2004). Nevertheless, coating though ionic interactions has been the basis of most of these methods.

In this part of the project, we developed a novel method of forming wet-spun chitosan-alginate hybridized fibers and analyzed their mechanical and morphological properties through dynamic mechanical analyzer (DMA), scanning electron microscopy (SEM) and optical microscope. Total nitrogen analysis was also included in order to calculate the chitosan content of the hybrid fibers.

3.2 EXPERIMENTAL

3.2.1 Materials

Commercial low molecular weight chitosan (average M_w=150,000 Da and deacetylation degree (DD) 80%) was supplied by Fluka. Commercial sodium alginate was purchased from Fisher Scientific. Sodium chloride (NaCl) and glacial acetic acid (CH_3COOH) was purchased from Fisher Scientific.

Syringe pump was supplied by Fisher Scientific. Syringes were purchased from HSW (Henke Sass Wolf), and needles were supplied by Becton Dickinson. All the materials were used as received.

3.2.2 Methods and Techniques

3.2.2.1 Chitosan solution preparation

Low molecular weight (LMW) chitosan powder was introduced into distilled water and next acetic acid was then added during the mixing process in order to reach 0.5 w/v% concentration. The chitosan dissolution process was carried out at a temperature of 20°C. The solution was also filtered through a 325 mesh stainless steel woven disk filter to remove the undissolved matter. After filtration, the pH of the chitosan solution was measured as 4.2 ± 0.1. The chitosan solutions prepared were used after suitable fragmentation via sonication for the process of forming the alginate-chitosan fibers.

3.2.2.2 Ultra-Sonication

Sonication is a simple technique that uses high-intensity acoustic energy to agitate particles in a sample for various purposes. In this project, sonication was used in order to reduce the molecular weight of low molecular weight chitosan (≈150 kDa). The probe of sonicator was dipped into chitosan solution and sonication was applied at high amplitude (40%) for a short period of time (20 min).

3.2.2.3 Determination of the average molecular weight of chitosan

The average molecular weights of non-treated and sonicated chitosan were determined by the viscometric method on the basis of intrinsic viscosity [η]. The determination of the intrinsic viscosity as a function of the concentration was performed with an Ubbelohde capillary viscometer (Ø = 0.58 mm) having a solvent flow time of at least 100 s. Solutions for viscometric measurements of the molecular weight of chitosan were prepared by a standard procedure (Pogodina et al., 1986). First, weighed portions of chitosan were dissolved in 0.33 M CH_3COOH. Then, NaCl was added up to a

concentration of 0.3 mol/l to suppress the polyelectrolyte effect. The solutions were passed through a filter of 325 mesh stainless steel woven disk to remove insoluble materials.

The capillary viscometer was filled with 10 ml of the sample and equilibrated in a water bath which was controlled with a thermostat to maintain the temperature at 21°C. Each sample was run 5 times. The running times of the solution and solvent were taken to calculate the kinematic viscosity. Kinematic viscosity can be converted to dynamic viscosity through:

$$\nu = \eta/\rho \qquad \text{(Equation 3.1)}$$

In this equation ν is the kinematic viscosity in stokes; η is the dynamic viscosity in poise; and ρ is the density in g/cm^3. Because the concentrations are low and the density of the solution and solvent are adjacent to 1 g/cm^3, the stoke (centistoke) is equal to poise (centipoise). The solution and solvent viscosities are used to calculate the relative viscosity, specific viscosity, reduced viscosity, and inherent viscosity on Equation 3.2, 3.3, 3.4 and 3.5 (Launay et al., 1986, Chen and Tsaih, 1998). The value of the intrinsic viscosity [η] was determined by the mean intercept of Huggins and Kraemer plots, using the Huggins and the Kraemer equation (Equation 3.6 and 3.7).

Relative viscosity $(\eta_{rel}) = t/t_s$ (Equation 3.2)

Specific viscosity $(\eta_{sp}) = \left(\frac{t}{t_s}\right) - 1$ (Equation 3.3)

Reduced viscosity $(\eta_{red}) = \eta_{sp}/c$ (Equation 3.4)

Inherent viscosity $(\eta_{inh}) = (\ln \eta_{rel})/c$ (Equation 3.5)

Huggins equation $\frac{\eta_{sp}}{c} = [\eta] + k_H[\eta]^2 c$ (Equation 3.6)

Kraemer equation $\frac{ln\,\eta_{rel}}{c} = [\eta] - k_K[\eta]^2 c$ (Equation 3.7)

where t is the running time of the chitosan solution, t_s is the running time of the solvent, c is the chitosan concentration in [g/dl] and k_H and k_K are the Huggins and Kraemer constants, respectively.

The values of viscosity average molecular weight (M_v) were calculated according to the Mark-Houwink equation:

$[\eta] = K M_v^a$ (Equation 3.8)

where K and a are constants for measurements, $K = 3.41\times10^{-5}$, $a = 1.02$ (Pogodina et al., 1986). These values of the constants were chosen due mainly to appropriateness in respect of the deacetylation degree (DD) of chitosan Pogodina et al. (1986) used and molecular weight range, 13-193 kDa.

3.2.2.4 Preparation of the sodium-alginate spinning solution

The sodium-alginate spinning solution (1% w/v) was prepared by dissolving sodium alginate powder in distilled water. The solution then was filtered through a 325 mesh stainless steel woven disk filter to remove the undissolved matter. After filtration, pH of the solution was measured as 7.2 ± 0.1.

3.2.2.5 Formation of the alginate-chitosan fibers

The sodium-alginate spinning solution, after filtration, was sucked into a plastic syringe with a 10 ml volume. Then, the determined amount of the solution was fed by a syringe pump through the selected needle into chitosan solution at a flow rate of 3.0

ml/min. (Figure 3.1). 30 G needle which has 0.16 mm inner diameter was used for the process.

The spinning solution was pressurized into chitosan solution to generate chitosan-alginate fiber. The solution gelled after mixing with chitosan solution at the needle outlet. After the gels grew into a round piece with ~1 mm^3 size, the gelled piece was pulled up with a pair of fine tweezers to let the stream of the spinning solution flow in a fiber shape.

Figure 3. 1 An illustration of the fiber formation

Fibers in gel state were retained in chitosan solution for different periods of time (1, 3, 6, 12, 24 hours). After collected from coagulation bath, each fiber was soaked in distilled water in order to remove the excess chitosan. They were finally left to dry at 30^{o}C in a convection oven.

If one inquiries the necessity of reducing the molecular weight of chitosan, our motive was to incorporate more chitosan into fibers. Initially, the fibers composed of non-treated chitosan (M_w = 150 kDa) and sodium alginate were also produced by drawing the gelled piece at the tip of the needle unlike the fibers which are formed simultaneously in the chitosan solution of reduced molecular weight. The former type of fibers was not uniform and had weak points which negatively affected the stability of the process of the formation of that fiber (Figure 3.2). This effect occurred most likely due to the misalignment of two polymers during micro-fluidic formation.

Figure 3. 2 Fiber produced with non-treated chitosan solution

The formation of the latter type of fiber is very similar to that of cross-linked either chitosan or alginate fiber. During crosslinking process, for example, sodium alginate solution is fed into calcium chloride solution bath whereby sodium alginate is precipitated out in filament form as a calcium alginate fiber. The Ca^{+2} ions (in our case

chitosan polymers) quickly diffuse into the gel solution and crosslink the polymer chains of alginate into a gel state through electrostatic force.

3.2.2.6 Diameter of fibers and the linear density

The diameters were measured on Spencer optical microscope made by American Optical Company [US]. 10 readings were taken randomly from 10 cm of each fiber and the average value of each fiber's diameter (Ø) was calculated and plotted against the retention time (Figure 3.3). For the calculation of the linear mass density of fibers, denier (Equation 3.9) was chosen as the unit. The density (ρ) of fibers is about 1.6 g/cm^3 since their main component is alginate.

$$denier = \frac{\pi}{4} * \left(\frac{Ø}{10^4}\right)^2 * \rho * (9 * 10^5) \qquad \text{(Equation 3.9)}$$

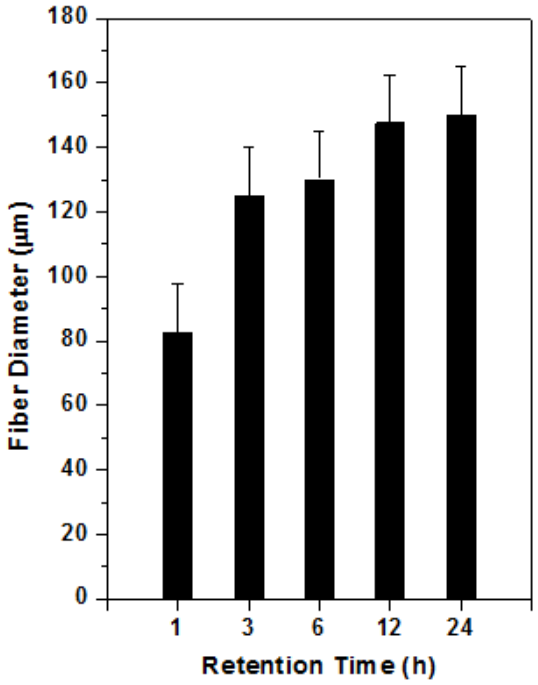

Figure 3. 3 The increase of the diameters of fibers with the retention time

3.2.2.7 Total nitrogen analysis

5 mg of 20 minutes sonicated chitosan powder which was collected by freeze drying method and the two fibers with 1h and 24 h retention time were sent to Atlantic Microlab, Inc. They performed the analyses by combustion using automatic analyzers. The test was aimed to determine the chitosan content of fibers from their nitrogen (N) contents.

3.2.2.8 Morphology analyses

The fractured cross section of the fibers pre-chilled in liquid nitrogen was studied by scanning electron microscope (SEM, Cambridge 360). Samples were sputtered with gold prior to SEM observation. Pictures of each fiber were taken under optical microscope that is also used for the measurement of diameters of fibers. Longitudinal roughness (R_a) and circumferential roughness (R_a) were measured on those pictures by an SPM data visualization and analysis computer program [Gwyddion].

3.2.2.9 Mechanical properties

Tensile tests were performed using a Dynamic Mechanical Analyzer (DMA RSA3 TA) Instrument on multiple extension mode, at room temperature (23°C ± 2°C). The initial length of fiber sample was 20 mm. It was clamped between grips and stretched by top grip at a rate of 0.05 mm/sec. The yield strength (σ_y), elongation at break (ε_b) and elastic modulus (*E*) and tenacity were calculated according to the ASTM D-3822-07 Standard Test Method for Tensile Properties of Single Textile Fibers (2007).

3.3 RESULT AND DISCUSSION

3.3.1 Average molecular weight of chitosan

Figure 3.4 and Figure 3.5 show Huggins/Kraemer plots of chitosan solutions which were used to calculate the [η] values. Using Mark-Houwink equation (Equation 3.8), viscosity average molecular weights were obtained (shown in Table 3.1).

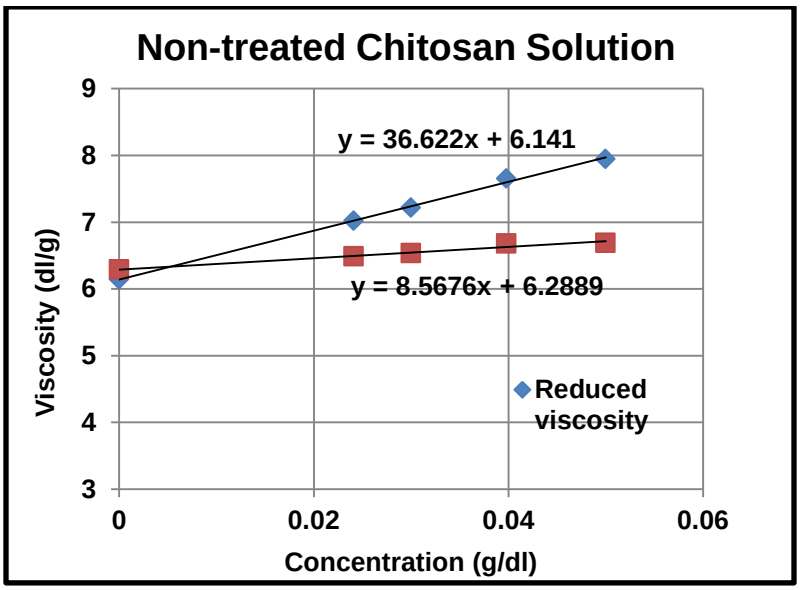

Figure 3. 4 Huggins and Kraemer plot of non-treated chitosan solution

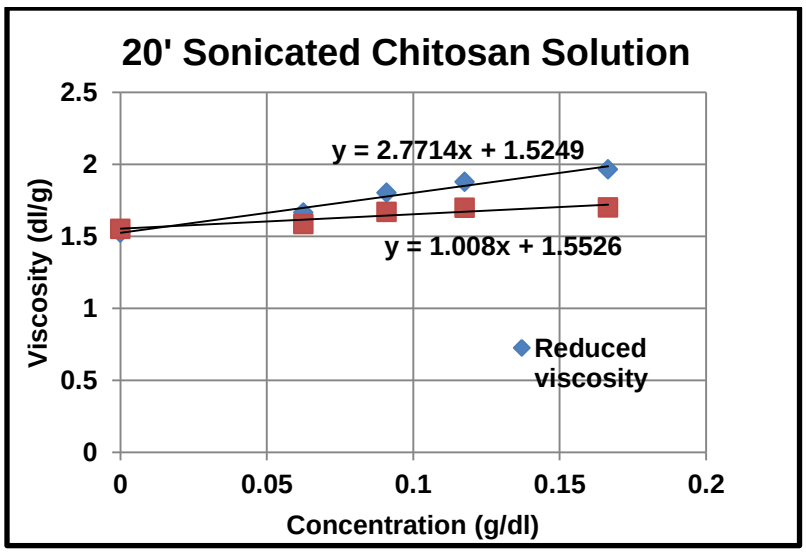

Figure 3. 5 Huggins and Kraemer plot of 20 min. sonicated chitosan solution

Table 3. 1 Viscosities and molecular weights of chitosan solutions

	η_{int} **intrinsic viscosity (dl/g)**	M_v **viscosity average (kDa) (Experimental data)**	M_w **weight average (kDa) (provided by Fluka, USA)**
Non-treated chitosan solution	6.215	143.7	150
20' sonicated chitosan solution	1.54	36.6	-

The viscosity average molecular weight of non-treated chitosan was measured in order to confirm the accuracy of the method. The value of M_v of chitosan is very close to the value of weight average molecular weight (M_w) of chitosan reported by the selling company, Fluka USA (shown in Table 3.1). These experiments confirm the theoretical distribution of molecular weights since the various average molecular weights always rank in the order:

$$\overline{M_N} \leq \overline{M_v} \leq \overline{M_W} \leq \overline{M_Z} \leq \overline{M_{Z+1}} \leq \overline{M_4} \leq \cdots \qquad \text{(Equation 3.10)}$$

3.3.2 The chitosan content of fibers

The total nitrogen analysis was performed on chitosan–alginate fibers to determine their nitrogen content so as to determine the percentage by weight of chitosan in the chitosan-alginate fibers. The results are displayed on Table 3.2.

Table 3. 2 The chitosan content of fibers

Element	20' sonicated chitosan powder	Fiber with 1 hour retention time	Fiber with 24 hour retention time
Nitrogen (% w/w)	7.1	0.21	0.33
Chitosan (% w/w)	100	2.96	4.65

With more retention time in chitosan solution, it was already predicted that chitosan would penetrate more into the gelled fiber. The result obtained from the total nitrogen analyses supports this phenomenon; the fiber with 24 hour retention time contains 4.65 w/w% chitosan.

Tamura et al. (2002) produced a fiber with a highest chitosan content of 0.067 w/w%. Compared to their study, we were able to incorporate a lowest chitosan content of 2.96 w/w% with at least 1 hour retention time in chitosan solution. Even though the formation of our fibers was not based on a continuous system, chitosan was not coated along the length of the fibers but bonded to alginate polymer.

3.3.3 Morphological characteristics of fibers

It is well studied that the surface properties of scaffolds change the interaction between cell and material through modified surface chemistry and roughness (Yilgor et al., 2009). As potential fibers for biomedical applications, we measured the roughness of fibers on the optical microscope pictures. Table 3.3 shows values of the roughness on fibers. These values are quantitative measurement of the roughness which can also be observed qualitatively on the optical microscope pictures and the SEM images of

fibers (Figure 3.6 and 3.7). Both longitudinal and circumferential roughness increase with gradual retention time in chitosan solution and thus with the growth of the diameter of fibers.

Table 3. 3 Changes of roughness of the fibers in longitude and in circumference

Retention Time (h)	Diameter µm	R_a (nm) *longitudinal*	R_a (nm) *circumferential*
1	82.5	29.8	72.4
3	125	49.1	89.3
6	130	55.4	93.2
12	147.5	58.3	107.7
24	150	69.8	118.5

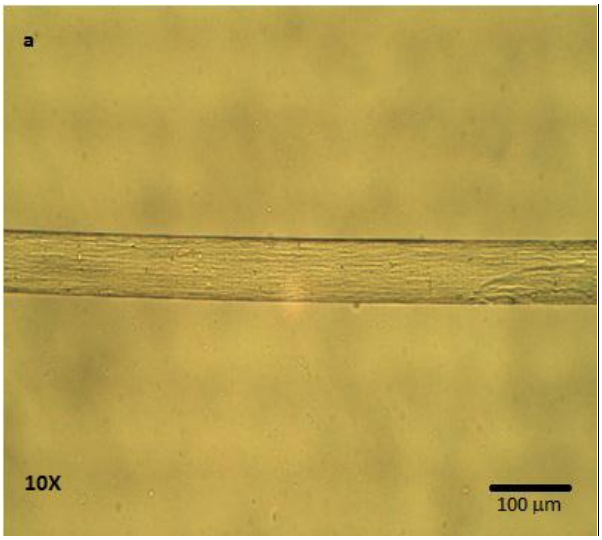

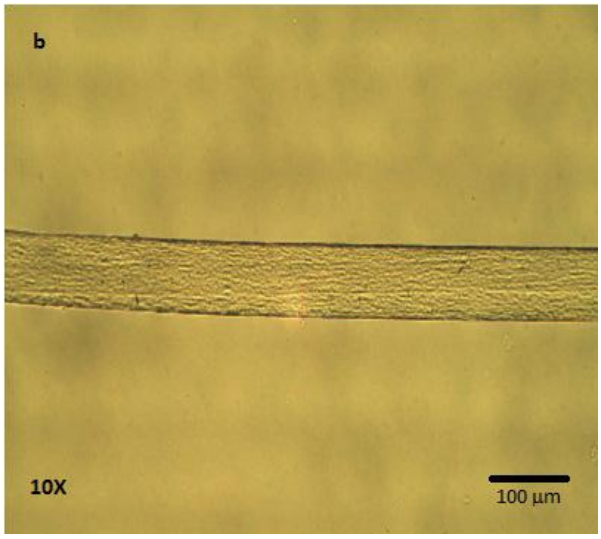

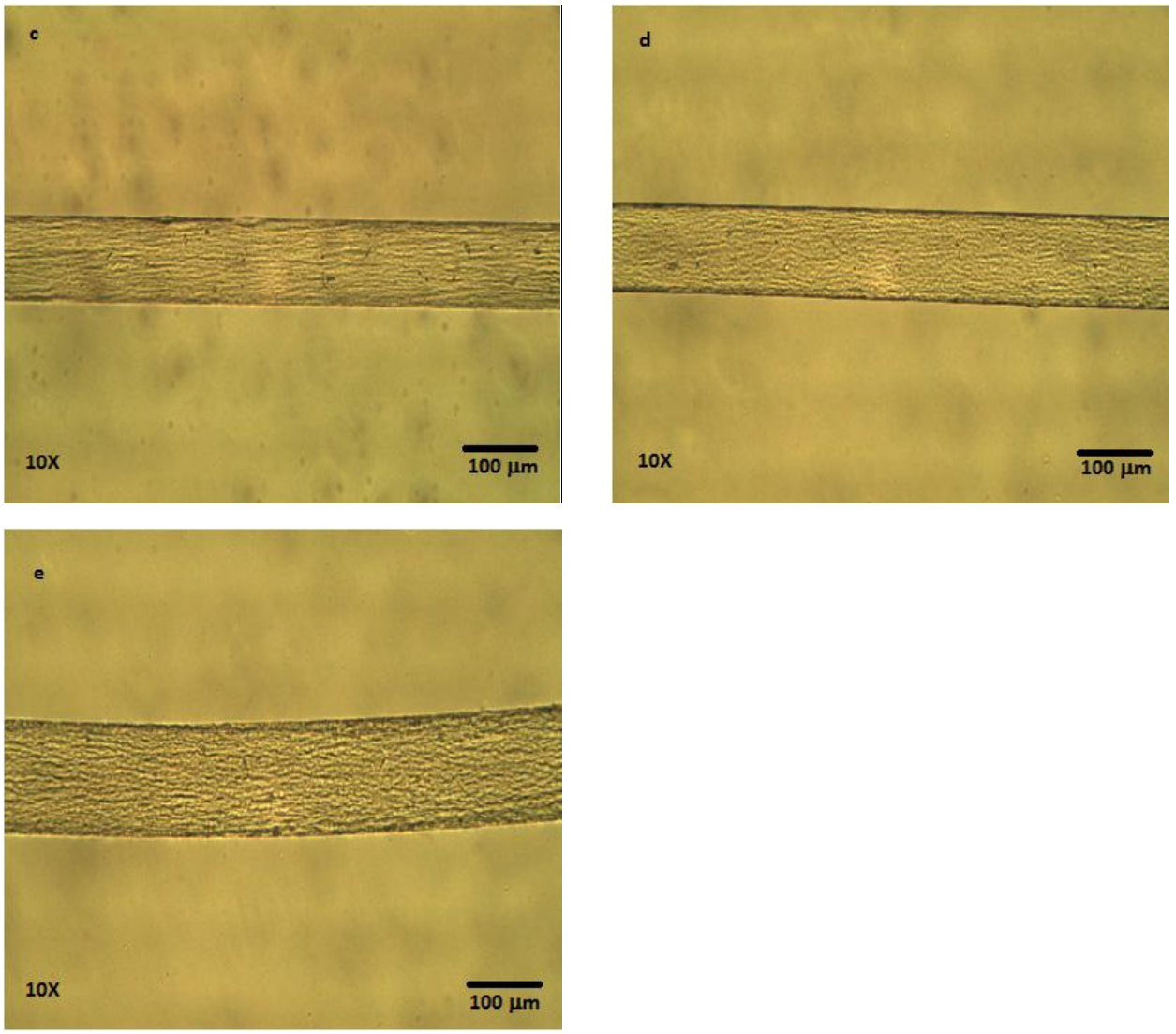

Figure 3. 6 Optical microscope pictures of fibers; a) 1h, b) 3h, c) 6h, d) 12h, e) 24h retention time

The diameter and the roughness of fibers (82.5 – 150 µm) were dependent upon the retention time in chitosan coagulation bath, suggesting more penetration of chitosan macromolecules into gel fiber. This was also confirmed with total nitrogen analysis of the hybrid fibers. The diffusion of chitosan into gel-state fiber occurred around the fiber creating slightly marked curved indentations. Figure 3.7 shows SEM pictures of surface

and cross section of fibers with different retention time. The surface of every fiber was characterized by distinct curved indentations, which were the main cause of roughness.

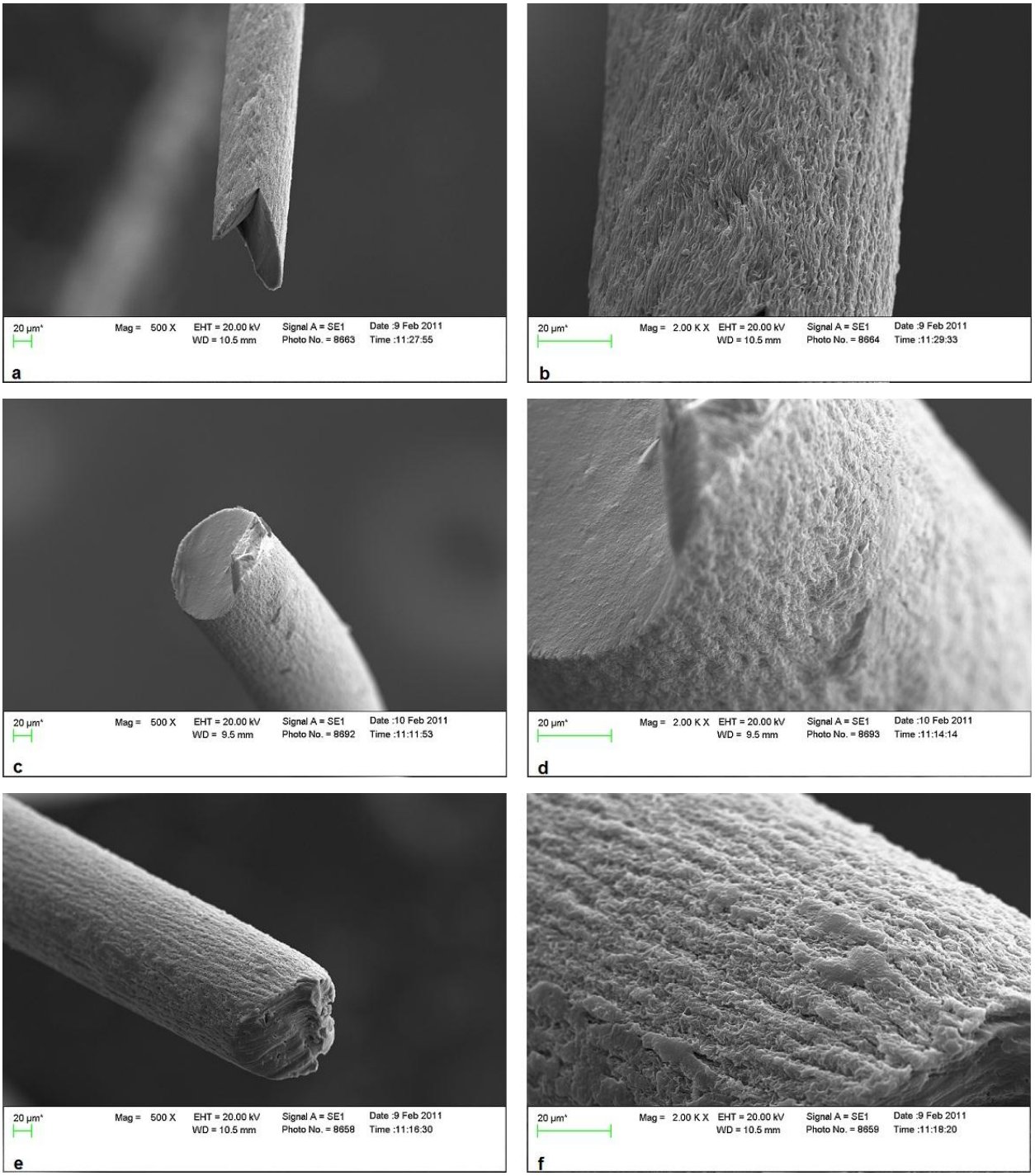

Figure 3. 7 Representative SEM images of surface of fibers coagulated with increasing retention time in chitosan solution; a, b) 1h, c, d) 12h, e, f) 24h

It is also important to emphasize that there is no coating of one polymer onto another. The cross section of fibers (Figure 3.7) shows no sign of layered or two phased structure but instead a hybridization of two polymers. It is also safe to assume that possible ionic interaction occurred through coupling of chitosan and alginate in the gel state of fibers. The coupled network of chitosan and alginate can be formed through heterotypic junction zones that bind them together.

3.3.4 Mechanical properties

Mechanical properties in terms of tenacity, elongation at break, and Young's modulus of all fibers were investigated and results are shown in Figure 3.8. All plots were drawn against the retention time (h) of the prepared samples in chitosan solution.

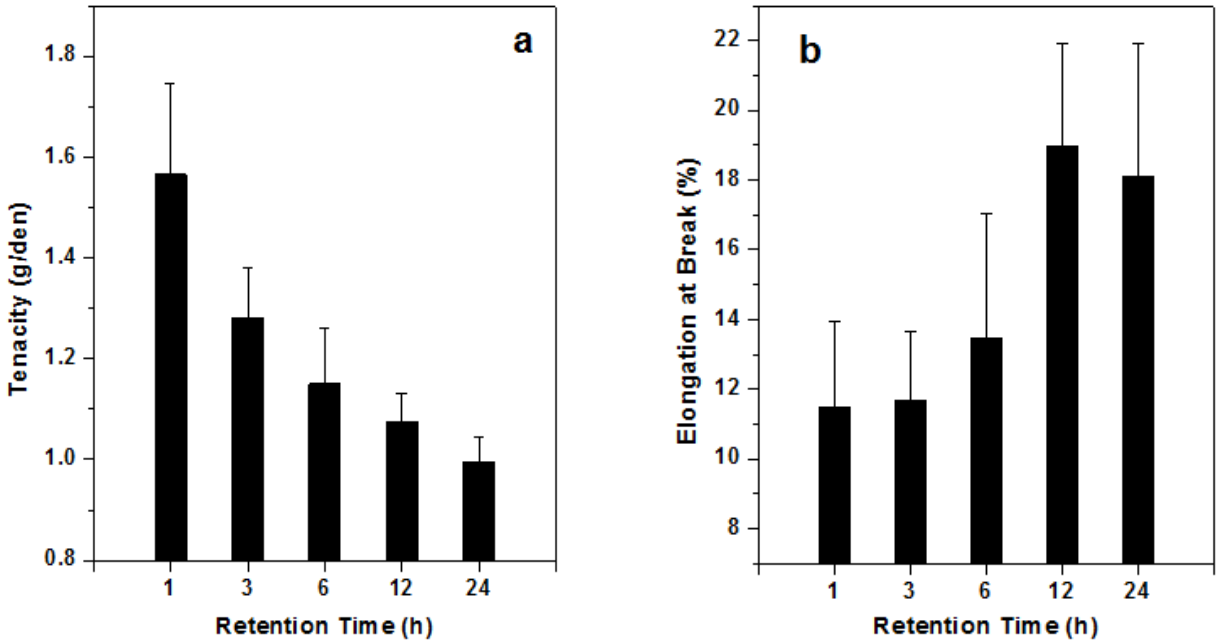

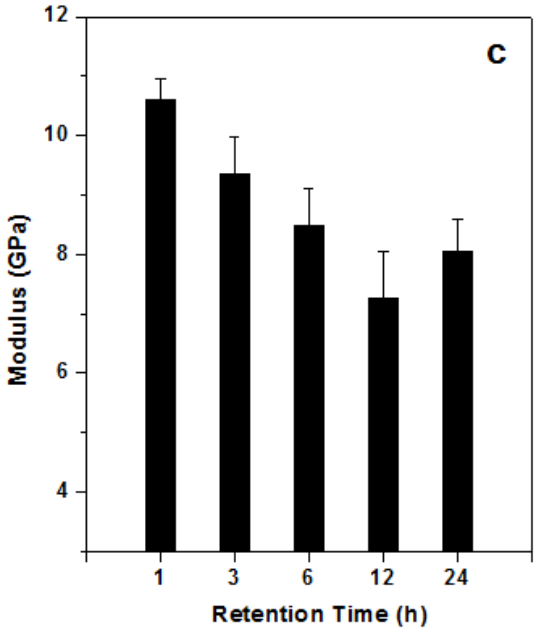

Figure 3. 8 a) Tenacity, b) Elongation at break and c) Young's modulus of fibers with increasing retention time

Clearly, higher retention times, in other words deeper penetration of chitosan into fibers, reduced modulus and tenacity in tensile tests, while it largely improved the ultimate deformation of fibers. Fibers became less rigid and more flexible and stretchable. Alternatively, lower modulus can be explained through the fracture behavior of the fiber with 24 hour retention time. Its SEM picture (Figure 3.7(e, f)) shows that its cross section is different from other fibers. So it can be concluded that additional incorporation of chitosan significantly changed the fracture behavior as well as the rigidity of fibers.

3.4 CONCLUSION

Fibers containing at least 2.96% of chitosan were obtained by a method for forming chitosan-alginate fibers which consisted in introducing alginate spinning solution into the chitosan coagulation bath. The formation of chitosan-alginate fibers consists of using chitosan solution with a reduced molecular weight, 36.6 kDa which was calculated through dilute solution viscometry.

Chitosan content of fibers completely depends on the retention time in chitosan solution. As the time increased so did the chitosan content. This also changed majorly morphology and mechanical properties of fibers.

The diameters of fibers enlarged with more inclusion of chitosan, also affecting surface morphology throughout the fiber. Roughness changed visibly and quantitatively in a gradual manner towards a higher degree. This can be observed in both optical microscopy and SEM pictures and confirmed with roughness measurements.

Mechanical properties in terms of modulus, tenacity and elongation at break were determined. The tensile results showed that the modulus and tenacity values were greatest at the lowest content of incorporated chitosan (i.e., 2.96 w/w% chitosan), while they decreased with a further increase in the chitosan content. But elongation at break values reversibly increased in the same manner of chitosan content.

REFERENCES

AOGREN, M. 1996. Four alginate dressings in the treatment of partial thickness wounds: a comparative experimental study. *British journal of plastic surgery,* 49**,** 129-134.

ASTM(D3822-07) 2007. Standard Test Method for Tensile Properties of Single Textile Fibers. *ASTM International.* Philadelphia, USA.

CHEN, R. H. & TSAIH, M. L. 1998. Effect of temperature on the intrinsic viscosity and conformation of chitosans in dilute HCl solution. *International journal of biological macromolecules,* 23**,** 135-141.

COLE, S. M. & NELSON, D. L. 1993. Alginate wound dressing of good integrity. Google Patents.

KENNEDY, J., PATERSON, M., KNILL, C. & LLOYD, L. The diversity of properties of polysaccharides as wound management aids and characterisation of their structures. Proceedings of the Fifth European Conference on Advances 1996 London. Wound Management, Macmillan Magazines, 122-126.

KENNEDY, J. F. & THORIEY, M. 2001. Natural polymers for healing wounds. *Recent Advances in Environmentally Compatible Polymers: Cellucon'99 Proceedings***,** 97.

KNILL, C., KENNEDY, J., MISTRY, J., MIRAFTAB, M., SMART, G., GROOCOCK, M. & WILLIAMS, H. 2004. Alginate fibres modified with unhydrolysed and hydrolysed chitosans for wound dressings. *Carbohydrate Polymers,* 55**,** 65-76.

KURITA, K., SHIMADA, K., NISHIYAMA, Y., SHIMOJOH, M. & NISHIMURA, S. I. 1998. Nonnatural branched polysaccharides: Synthesis and properties of chitin and chitosan having -mannoside branches. *Macromolecules,* 31**,** 4764-4769.

LAUNAY, B., DOUBLIER, J. & CUVELIER, G. 1986. Flow properties of aqueous solutions and dispersions of polysaccharides. *Functional properties of food macromolecules***,** 1-78.

LIAO, I. C., WAN, A. C. A., YIM, E. K. F. & LEONG, K. W. 2005. Controlled release from fibers of polyelectrolyte complexes. *Journal of Controlled Release,* 104**,** 347-358.

LLOYD, L., KENNEDY, J., METHACANON, P., PATERSON, M. & KNILL, C. 1998. Carbohydrate polymers as wound management aids. *Carbohydrate Polymers,* 37**,** 315-322.

NIEKRASZEWICZ, A. & CIECHA SKA, D. 2006. Research into the Process of Manufacturing Alginate-Chitosan Fibres. *FIBRES & TEXTILES in Eastern Europe,* 14**,** 58.

PANDIT, A. S. 1998. Hemostatic wound dressing. Google Patents.

POGODINA, N., PAVLOV, G., BUSHIN, S., MEL'NIKOV, A., LYSENKO, Y. B., NUD'GA, L., MARSHEVA, V., MARCHENKO, G. & TSVETKOV, V. 1986. Conformational characteristics of chitosan molecules as demonstrated by diffusion-sedimentation analysis and viscometry. *Polymer Science USSR,* 28**,** 251-259.

QIN, Y. 2008. Alginate fibres: an overview of the production processes and applications in wound management. *Polymer International,* 57**,** 171-180.

QIN, Y. & AGBOH, O. 1998. Chitin and Chitosan fibres: Unlocking their potential. *Medical device technology,* 9**,** 24-28.

TAMURA, H., TSURUTA, Y. & TOKURA, S. 2002. Preparation of chitosan-coated alginate filament. *Materials Science and Engineering: C,* 20**,** 143-147.

TUZLAKOGLU, K. & REIS, R. L. 2008. Biodegradable polymeric fiber structures in tissue engineering. *Tissue Engineering Part B: Reviews,* 15**,** 17-27.

WATTHANAPHANIT, A., SUPAPHOL, P., FURUIKE, T., TOKURA, S., TAMURA, H. & RUJIRAVANIT, R. 2009. Novel Chitosan-Spotted Alginate Fibers from Wet-Spinning of Alginate Solutions Containing Emulsified Chitosan−Citrate Complex and their Characterization. *Biomacromolecules,* 10**,** 320-327.

YILGOR, P., TUZLAKOGLU, K., REIS, R. L., HASIRCI, N. & HASIRCI, V. 2009. Incorporation of a sequential BMP-2/BMP-7 delivery system into chitosan-based scaffolds for bone tissue engineering. *Biomaterials,* 30**,** 3551-3559.